Effects of the Western Mediterranean Oscillation in the moisture transport from the Mediterranean Sea and the North Atlantic Ocean

Implications on precipitation patterns over the Iberian Peninsula and Europe

Master's Thesis

in Oceanography

Submitted to the
Faculty of Marine Science
University of Vigo

in Partial Fulfilment of the Requirements for the Degree of
Master of Science

by
Jakob Ernst

Advisors
Dr. Rogert Sorí Gómez
Dra. Milica Stojanovic

Vigo, July 2024

To Elisa, María, Rocío and the fantastic phenomenon of clouds made out of water and ice floating in the atmosphere.

Abstract

The Western Mediterranean Oscillation (WeMO) index is based on the atmospheric pressure differences between Northern Italy and southwestern Spain. This study aims to investigate the influence of the WeMO on the moisture contribution to precipitation from the subtropical North Atlantic Ocean (NALT) and the Mediterranean Sea (MEDT) over Europe and the Iberian Peninsula (IP). Therefore we tracked the air masses residing over these sources forward in time with the Lagrangian FLEXible PARTicle dispersion model (FLEXPART) for 39 years, between 1980-2018. Additionally, we used the WeMO index as well as precipitation and atmospheric moisture flux data. Results showed that during positive WeMO phases, precipitation increases over Europe from approximately 43°N to 60°N. In contrast, during negative WeMO phases, it increases over the central-southern IP and Norway. WeMO(+) also increases the moisture contribution from the MEDT to precipitation over Eastern Europe, while WeMO(-) increases the moisture contribution from the MEDT to precipitation over Western Europe. Regarding moisture transport from the NATL, during a WeMOi(+), a positive anomaly occurs over France, Central Europe, the Italian Peninsula, the Balkans, and Eastern Europe, while a negative anomaly is evident over southwestern Spain. Under WeMOi(-) conditions, the opposite characteristics are observed. The seasonal analysis revealed that for both MEDT and NATL, the anomalies in moisture contribution over Europe are more pronounced in autumn and winter, however, the sign pattern is similar during all seasons. Focusing on the analysis of the IP, we distinguished two different zones (northern and central-southern IP) of precipitation variability under WeMO(+/-) influence. Also, for the IP the NATL supplies a greater amount of moisture in comparison to the MEDT and the IP itself. However, moisture supply from the MEDT is the best correlated with precipitation. Besides, Extreme Precipitation (EP) events during a WeMO(+) are more frequent in the northern IP and during a WeMO(-) in the central-southern IP, particularly during winter. This study reveals for the first time the role of the WeMO in the transport of moisture from the MEDT and NATL over Europe, as well as its influence on the precipitation variability over Europe, and particularly EP over the IP. These results contribute to the understanding of the ocean-atmosphere interaction and thus of the hydrological cycle, providing important information that supports environmental and socio-economic activities.

Keywords: WeMO, Moisture transport, Precipitation, Extreme precipitation, Teleconnections, Mediterranean Sea, North Atlantic Ocean

List of Acronyms

The following abbreviations are used in this manuscript:

AO ...	Artic Oscillation
CDO ...	Climate Data Operators
CESGA ...	Centro de Supercomputación de Galicia
ENSO ...	El Niño-Southern Oscillation
EP ...	Extreme Precipitation
e ...	Evaporation
E ...	Vertically integrated Evaporation
FLEXPART ...	FLEXible PARTicle dispersion model
IP ...	Iberian Peninsula
IPCC ...	Intergovernmental Panel on Climate Change
q ...	Specific humidity
m ...	Mass
MEDT ...	Mediterranean Sea
NATL ...	North Atlantic Ocean
NAO ...	North Atlantic Oscillation
p ...	Precipitation
P ...	Vertically integrated Precipitation
VIMF ...	Vertically Integrated Moisture Flux
WeMO ...	Western Mediterranean Oscillation
WeMOi ...	Western Mediterranean Oscillation Index

Contents

Abstract iii

List of Acronyms v

Contents vii

1 Introduction 1
- 1.1 Motivation . . . 1
- 1.2 Western Mediterranean Oscillation (WeMO) . . . 3
- 1.3 Objective and Structure . . . 3

2 Material and Methods 5
- 2.1 Investigation area . . . 5
- 2.2 Data . . . 5
  - 2.2.1 E-OBS . . . 5
  - 2.2.2 Iberia01 . . . 6
  - 2.2.3 Eulerian data . . . 6
  - 2.2.4 Western Mediterranean Oscillation Index (WeMOi) . . . 7
  - 2.2.5 FLEXible PARTicle dispersion model (FLEXPART) . . . 7
- 2.3 Calculations . . . 8
  - 2.3.1 Trends and Correlations . . . 9
  - 2.3.2 Anomalies . . . 9
  - 2.3.3 Extreme precipitation identification . . . 9

3 Results and Discussion 11
- 3.1 Hydroclimate conditions over Europe . . . 11
- 3.2 Linear relationship assessment over Europe . . . 12
- 3.3 Hydroclimate anomalies during WeMOi(+/−) phases over Europe . . . 13
  - 3.3.1 Annual hydroclimate anomalies . . . 13
  - 3.3.2 Seasonal hydroclimate anomalies . . . 16
- 3.4 The Iberian Peninsula hydroclimate and the WeMO . . . 21
  - 3.4.1 The linear relationship distinguishes two zones . . . 22
  - 3.4.2 Moisture origin and the WeMO . . . 23
  - 3.4.3 Temporal evolution: Hydroclimate and the WeMO . . . 25
  - 3.4.4 Extreme precipitation . . . 27
  - 3.4.5 $|(\boldsymbol{E}-\boldsymbol{P})<\mathbf{0}|$ for extreme precipitation and the WeMO . . . 32

4 Conclusions **37**

Acknowledgments **39**

Bibliography **41**

Supplementary Material **49**

Chapter 1

Introduction

1.1 Motivation

Global evaporation from oceanic and terrestrial regions is crucial for the global hydrological cycle, with oceans supplying more than 85% of atmospheric water vapour and serving as major sources of moisture for rainfall (Oki and Kanae 2006; Gimeno et al. 2010a). Figure 1.1 summarises the evolution of the hydrological cycle. It reveals the existence of the components that act as sources of moisture through oceanic and terrestrial evaporation and transpiration, as well as the processes of atmospheric moisture removal through precipitation. Thus, gaining knowledge about the atmospheric branch of the hydrological cycle, particularly the atmospheric moisture transport, leads to a better understanding of precipitation variability and extremes, at local (Benetó and Khodayar 2023), regional (Horan et al. 2023; Sorí et al. 2023), and global scales (Yang et al. 2022).

Indeed, investigating the relationship between sources and sinks of atmospheric sources represents a challenge for atmospheric sciences (Gimeno 2013; Soden 2019; Ma et al. 2020). This is why several methodologies and techniques (Eulerian, Lagrangian, isotopes) have been developed for their study (Gimeno et al. 2012). Multiple studies have performed evaluations about the source and sinks of atmospheric water vapour, including its role in the occurrence of extreme precipitation (Liu et al. 2020), droughts (Herrera-Estrada and Diffenbaugh 2020; Gimeno-Sotelo et al. 2024a) and tropical cyclones (Pérez-Alarcón et al. 2022).

The source-sink relationship allows us to identify the sources of moisture for the precipitation in a target region. Following this criteria, the subtropical North Atlantic Ocean (NATL) and the Mediterranean Sea (MEDT) have been identified as the major oceanic sources for precipitation over Europe and the Iberian Peninsula (Gimeno et al. 2010a,b; Nieto et al. 2014).

So far, the role of various modes of variability, such as the North Atlantic Oscillation (NAO), the El Niño-Southern Oscillation (ENSO), the Arctic Oscillation (AO) and others, in the climate of the Iberian Peninsula (IP) and Europe in general has been extensively studied considering their role on atmospheric patterns changes (Lopez-Bustins et al. 2008; Castillo et al. 2014), moisture transport (Ordóñez et al. 2013; Martinez-Artigas et al. 2021; Vázquez et al. 2023) and precipitation variability

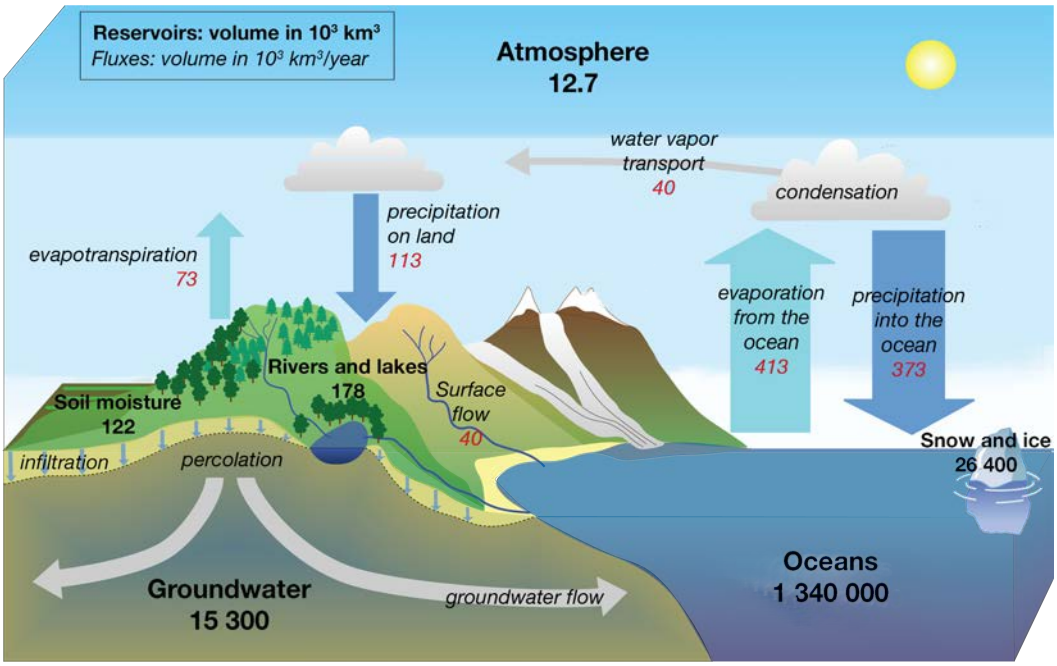

Figure 1.1: Schematic illustration of the hydrological cycle. Red/black numbers represent fluxes/reservoirs. Figure adjusted from Egger (2003).

(Casanueva et al. 2014; Shaman 2014; Martinez-Artigas et al. 2021). Particularly, the Western Mediterranean Oscillation (WeMO) has mainly been studied over the IP (Martin-Vide and Lopez-Bustins 2006; Lopez-Bustins et al. 2008; Martinez-Artigas et al. 2021) and has been related to the occurrence of extreme precipitation over Spain (Merino et al. 2016), and particularly Cataluña (Lopez-Bustins et al. 2020). However, this index represents pressure variations and mass movements that influence the general circulation over the Iberian Peninsula (Martin-Vide and Lopez-Bustins 2006; Merino et al. 2016; Martinez-Artigas et al. 2021) and parts of Europe. The effects of these changes in the moisture transport and contribution to rainfall from the main moisture sources (NATL and MEDT) to precipitation over Europe and the IP have not been studied, which initially motivated the choice of this topic as a Master's Thesis. A description of this mode of variability is given in the next section 1.2.

According to the Intergovernmental Panel on Climate Change (IPCC), the frequency and intensity of heavy precipitation events have likely increased at the global scale over a majority of land regions with good observational coverage, particularly North America, Europe, and Asia (Seneviratne et al. 2021). This report also confirmed with medium confidence that human-induced climate change has contributed to increased agricultural and ecological droughts in some regions like the Mediterranean. Furthermore, it has been proved that climate change affects moisture transport and precipitation (Watterson 2023). As the Mediterranean is a changing hot spot (Cos et al. 2022; Lopez-Bustins and Lemus-Canovas 2020; Insua-Costa et al. 2022), the WeMO

teleconnection is also likely to change. Thus, unravelling the processes and mechanisms responsible for controlling the variability of precipitation is an advantage for the development of policies. Policies, which help to be prepared for extreme hydrometeorological events, which cause considerable damage to infrastructure, agriculture, ecosystems, and society in general. This is of great importance for densely populated and industrially developed regions such as Europe.

1.2 Western Mediterranean Oscillation (WeMO)

The Western Mediterranean Oscillation (WeMO) is described as the surface pressure difference between the Po Plain (Padua, Italy) and the Gulf of Cádiz (San Fernando, Spain). This oscillation affects the Western Mediterranean basin, and the San Fernando-Padua line describes a parallel to the northwestern border of this basin. Therefore, the WeMO is a crucial factor for the weather and climate over the Iberian Peninsula (IP) and Europe. A positive index is driven by a pronounced Genoa low-pressure system and an Azores Anticyclone, inducing a northwesterly atmospheric flow over the IP. Conversely, a negative index, associated with a low above the Gulf of Cádiz and a high over Central to Eastern Europe, results in a southeasterly atmospheric flow (Martin-Vide and Lopez-Bustins 2006; Lopez-Bustins and Lemus-Canovas 2020)

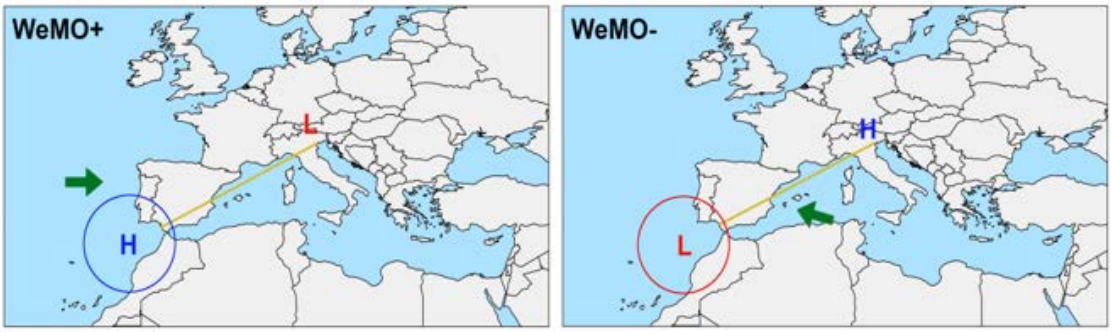

Figure 1.2: Schematic illustration of the positive (left) and negative (right) WeMO phases. Green arrows represent the flow direction.

Figure 1.3 shows the temporal evolution of the WeMO for the 1980-2018 period. It reveals that the WeMO experienced a statistically significant negative trend during the study period. The visual analysis permits us to conclude that the prevalence of negative values occurred from 2003 onwards.

1.3 Objective and Structure

Taking into account the issues mentioned in section 1.1, the main objective of this Master's Thesis is to investigate the influence of the WeMO on the moisture transport patterns that contribute to precipitation over Europe, from its main source regions,

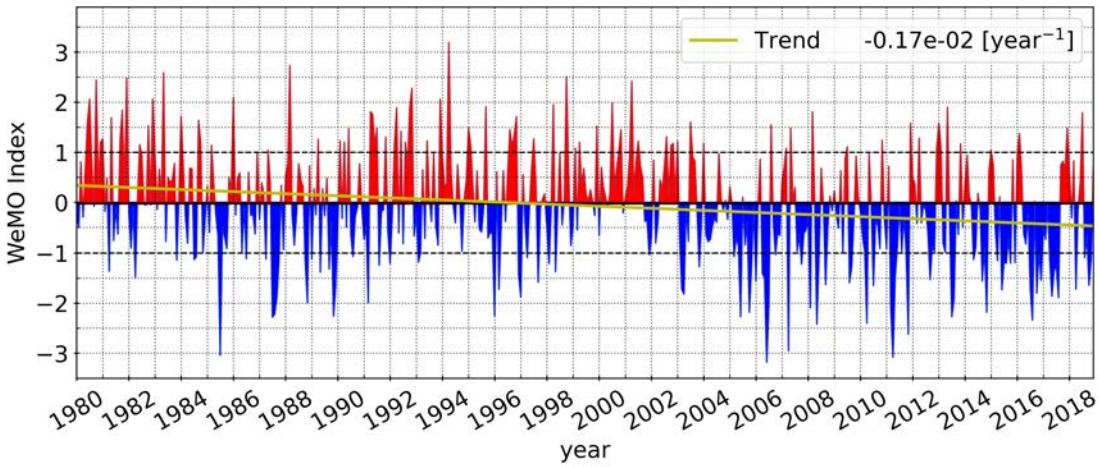

Figure 1.3: Monthly values of the WeMOi. Period: 1980-2018. Red/blue indicates positive/negative values, higher/lower black dotted lines indicate thresholds for WeMOi positive/negative phases, and the yellow line represents the linear trend line.

which are the North Atlantic Ocean and the Mediterranean Sea. In addition, a more specific objective is to determine the influence of changes in the contribution of moisture transported from these sources under opposite phases of the WeMO on precipitation patterns over the Iberian Peninsula, specifically on extreme precipitation.

This Master's Thesis is structured as follows: Chapter 2 outlines the investigation area, the data, and the methodology applied, Chapter 3 presents and discusses the results, zooming in from Europe all the way to the Iberian Peninsula, and finally, Chapter 4 provides the conclusion. Acknowledgements, bibliography, and supplementary material follow.

Chapter 2

Material and Methods

2.1 Investigation area

The climatological research of moisture transport variations under WeMO influences is focused on Europe, while a deeper analysis related to precipitation changes is performed for the IP. Figure 2.1 illustrates the boundaries and spatial extension of the subtropical North Atlantic Ocean (NATL), the Mediterranean Sea (MEDT), and the IP area moisture sources, in red, blue and green respectively. In this study, the Mediterranean Sea was considered in its entirety given previous work that also confirmed its importance as a source of moisture for precipitation over Europe (Gimeno et al. 2010a; Nieto et al. 2014, 2019) and the IP (Nieto et al. 2010), especially in summer (Gimeno et al. 2011). However, the source of the NATL was spatially defined using 0.1 mm day^{-1} in the $(E - P) > 0$ field as a limit, obtained in a backward in time analysis of air masses residing over the IP, using the FLEXPART model (section 2.2.5). This area of the NATL agrees with that defined in a previous experiment and is estimated as the major moisture source, from the entire North Atlantic Ocean, which contributes to humidity loss over the IP (Gimeno et al. 2010b). In addition, for the analyses of the precipitation changes over the IP, its area was added as a moisture source. This was done to further analyse the moisture recycling component of the IP besides the moisture supply from the MEDT and NATL.

2.2 Data

In order to relate the moisture contribution (calculated with data from FLEXPART 2.2.5) with precipitation, daily precipitation data from E-OBS 2.2.1 and Iberia01 2.2.2 were used, for Europe and the IP respectively. Additionally, the Eulerian data 2.2.3 were used to analyse and support the Lagrangian results from FLEXPART and monthly WeMOi 2.2.4 to classify the WeMO positive and negative phases.

2.2.1 E-OBS

The E-OBS dataset is an ensemble daily gridded observational precipitation, temperature, sea level pressure, relative humidity, global radiation and wind speed dataset over Europe. The dataset also provides the ensemble mean (best guess value) of 20

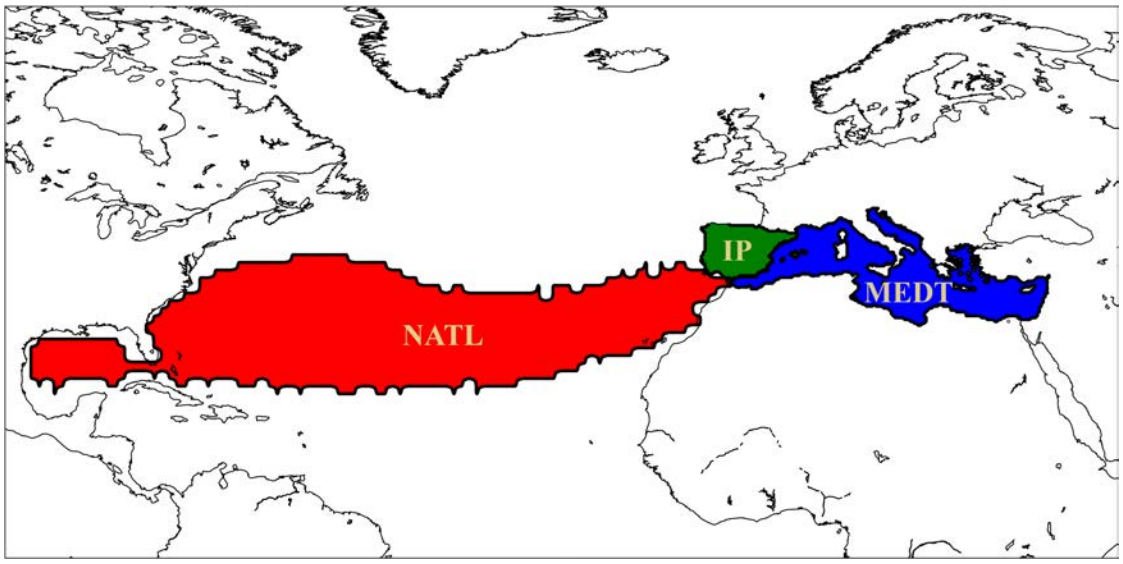

Figure 2.1: Geographical extension of the subtropical North Atlantic Ocean (NATL), in red, and the Mediterranean Sea (MEDT), in blue and the Iberian Peninsula (IP), in green, moisture sources considered for this study.

ensemble members (differently gridded observed datasets). A horizontal resolution of 0.25° and version 28.0e was chosen, which includes daily data from January 01, 1950 to June 30, 2023 (Cornes et al. 2018). For Europe, a monthly mean of precipitation data from 1980 to 2018 was calculated using Climate Data Operators (CDO) software (Schulzweida 2023) from the Max Planck Institute of Meteorology.

2.2.2 Iberia01

To focus the assessment on the influence of the moisture contribution to precipitation from the Mediterranean and the North Atlantic sources to the precipitation over the IP, the Iberia01 dataset (Herrera et al. 2019) for the period 1980-2015 was used. It is a daily gridded observational dataset for precipitation and temperature with a horizontal resolution of 0.1° from 1971 to 2015. This dataset was chosen because it provides better results in the representation of the precipitation over complex orographic areas of the IP compared to the E-OBS data, due to a dense network of stations (Herrera et al. 2019).

2.2.3 Eulerian data

The vertically integrated northward and eastward water vapour flux and the vertically integrated divergence of the moisture flux from the ERA 5 reanalysis database (Hersbach et al. 2023) were used to calculate the resulting vector, hereafter named VIMF (Vertically Integrated Moisture Flux), and its divergence. These fields provide a Eulerian perspective of moisture transport in the atmosphere and support the under-

standing of atmospheric moisture transport diagnosed by the Lagrangian FLEXPART model (Gimeno et al. 2010b, 2012).

2.2.4 Western Mediterranean Oscillation Index (WeMOi)

To classify the WeMO phases, the monthly WeMO index (WeMOi) from Martin-Vide and Lopez-Bustins (2006) was utilised. This index describes the difference between San Fernando (Spain) and Padua (Italy) in the standardised atmospheric surface pressure (Martin-Vide and Lopez-Bustins 2006). Following Martin-Vide and Lopez-Bustins (2006), the thresholds ≥ 1 and ≤ -1 were chosen for the positive and negative phases of the WeMOi, respectively. A more detailed explanation of the characteristics of this mode of climate variability was provided in section 1.2. The WeMOi was used for the years 1980-2018 for Europe and from 1980 to 2015 to analyse the precipitation patterns over the IP.

2.2.5 FLEXible PARTicle dispersion model (FLEXPART)

The FLEXible PARTicle dispersion model v9.0 (FLEXPART) (Stohl and James 2004, 2005) is a Lagrangian model originally designed for the analysis of pollutant transport. However, it has been widely used to track atmospheric parcels and to compute the changes in specific humidity along their trajectories. This has made it possible to study the atmospheric branch of the global hydrological cycle and to identify sources and sinks of moisture. In this study the atmosphere was divided into approximately 2 million parcels with the same mass and 1° of horizontal resolution, using the input data from the ERA-Interim Reanalysis project (Dee et al. 2011) with a temporal step of 6 hours and 61 vertical levels, as in recent studies that implemented the same methodology (Devanand et al. 2024; Gimeno-Sotelo et al. 2024b).

To calculate the moisture contribution from the NATL and MEDT sources to precipitation over Europe and particularly over the IP, a forward analysis was conducted. This involved tracking forward in time the air masses residing over the sources in time intervals of 6 hours up to 10 days, considering the mean water vapour residence time in the atmosphere (Numaguti 1999; Quante and Matthias 2006; Gimeno et al. 2021). The advection of air parcels mainly consists of a "zero acceleration" scheme that solves the trajectory equation 2.1,

$$\frac{dx}{dt} = v(x(t)) \tag{2.1}$$

where dx is the position of the parcel and $v(x(t))$ is the spatial and temporally interpolated wind speed. The gain (through evaporation from the environment, e) or loss (through convection and precipitation, p) of the specific humidity (q) by each parcel is

calculated following equation 2.2.

$$(e - p) = m\frac{dq}{dt} \tag{2.2}$$

Where $(e - p)$ represents the budget of evaporation minus precipitation in each parcel, m the mass, and $\frac{dq}{dt}$ the changes in time of the specific humidity. The values of $(e - p)$ integrated over the entire vertical column are represented as the balance of $(E - P)$, where E represents the total evaporation and P represents total precipitation, allowing us to estimate the freshwater balance at the surface.

Areas with positive values of $(E - P)$ in a backward experiment from a target region indicate that air masses uptake humidity, and represent a source region. This approach was utilised to determine the spatial extension of the North Atlantic Ocean moisture source (NATL) contributing to the precipitation over the IP, considering the threshold of 0.1 mm day^{-1}. In contrast, in a forward in time experiment from a target region, the areas where $(E - P) < 0$ indicate a contribution to precipitation from the air masses residing over that target region. The module of this balance sheet will be applied to facilitate the process of understanding the results. The patterns of $(E - P) < 0$ in [mm day^{-1}] were determined from a forward experiment of each source (NATL, MEDT, IP) and interpolated to a 0.25° grid resolution. Moreover, to investigate the relationship of the $|(E - P) < 0|$ values with the precipitation according to Iberia01 data, these datasets have been further interpolated to the same resolution as the latter, 0.1°, using CDO.

Lagrangian methods for tracking moisture transport have been highly recommended (Dirmeyer and Brubaker 1999, 2006). FLEXPART, in particular, is characterised by several strengths, such as its capacity to establish a source-receptor relationship and the net freshwater flux estimation that gives a realistic representation of the atmosphere water budget (Stohl and James 2004, 2005). However, evaporation rates are based on calculations rather than observations, and evaporation and precipitation are not clearly separable. Despite these negative aspects of FLEXPART, in general, they do not limit the use of the model and its results for the study of the atmospheric branch of the hydrological cycle.

2.3 Calculations

All the calculations were done in Python (Van Rossum and Drake 2009) and CDO (Schulzweida 2023). The libraries primarily used included: *xarray, numpy, pandas, scipy, netCDF4* and *datetime*.

2.3.1 Trends and Correlations

To calculate the temporal trends (slopes) and the correlations (Pearson correlation coefficient), a linear least-squares regression between time and the data or two datasets was used. Therefore the *scipy.stats* package in Python was used (Virtanen et al. 2020). Additionally, to determine the significance of the results, the p value was calculated using the Wald Test with a t-distribution of the test statistic (Virtanen et al. 2020). All results were classified as statistically significant if the p value was smaller than 0.05.

2.3.2 Anomalies

Anomalies were calculated by determining the temporal mean of each grid cell and subtracting this mean from the respective values of each grid cell. For monthly anomalies, the mean was taken over the corresponding month, regardless of different WeMO phases. To get the seasonal anomaly, the seasonal mean of the monthly anomaly was calculated

2.3.3 Extreme precipitation identification

To identify the area and days with Extreme Precipitation (EP) from the Iberia01 dataset, the R99p index was used. This index describes the values of daily precipitation exceeding the 99th percentile of the rainy days (days with precipitation equal or greater than 1 mm day^{-1}), calculated for each grid cell throughout the study period (1980-2015). The 99th percentile indicates the value below which 99% of the data points fall. In other words, if you have a sorted list of data, the 99th percentile is the value that separates the highest 1% of the data from the rest. Values exceeding the 99th percentile were marked as EP. This method has been used in several studies (e.g. Merino et al. 2016; Gimeno et al. 2022). The 99th percentile was calculated with the *numpy.percentile* function in the programming language Python.

Chapter 3

Results and Discussion

3.1 Hydroclimate conditions over Europe

To start our analysis, the spacial mean precipitation and mean $|(E-P)<0|$ from the MEDT and NATL over Europe are shown in figure 3.1. Areas with the highest precipitation values are found over the Atlantic coast of Norway, Northern Great Britain, the Alps, the Balkans, the northwestern IP and the eastern coast of the Black Sea. Most of Europe, except Mediterranean areas, are favoured by moist climate conditions because of higher average precipitation than evapotranspiration rates (Ullah et al. 2022; Luo et al. 2023), although the European countries have been confronting water stress (European Environment Agency 2021).

Concerning the moisture contribution from the MEDT source, the major values are observed over the Mediterranean and Eastern Europe, with its peak values south of the Alps, over the Balkans and the eastern coast of the MEDT, in agreement with the findings of Batibeniz et al. (2020). However, the NATL contributes the most moisture to the precipitation over Western Europe, specifically over Great Britain, the Western IP, France and Central Europe, as demonstrated in previous studies (e.g. Smith et al. 2016; Wypych et al. 2018; Fernández-Alvarez et al. 2023). These patterns can explain the higher mean precipitation values, except for Norway and the east of the Black Sea. A stronger influence on the precipitation over Norway from sources further north than the subtropical North Atlantic Ocean (NATL) can explain the non-representation of the strong mean precipitation from our sources, as appreciated in the results of Nieto et al. (2014). It can also be assumed that the high precipitation values east of the Black Sea are favoured by moisture transport from the Black Sea itself, which was found by Önol et al. (2014), Kozachek et al. (2017) and Batibeniz et al. (2020) for the summer.

Thus, observing these results in combination with the correlation from figure 3.2, the WeMO has an important impact on the moisture transport patterns and the precipitation over great parts of Europe, especially the IP, France, Central Europe, the Balkans and eastern and southeastern Europe. In section 3.3 we will have a closer look at how the WeMO influences the hydroclimate over Europe.

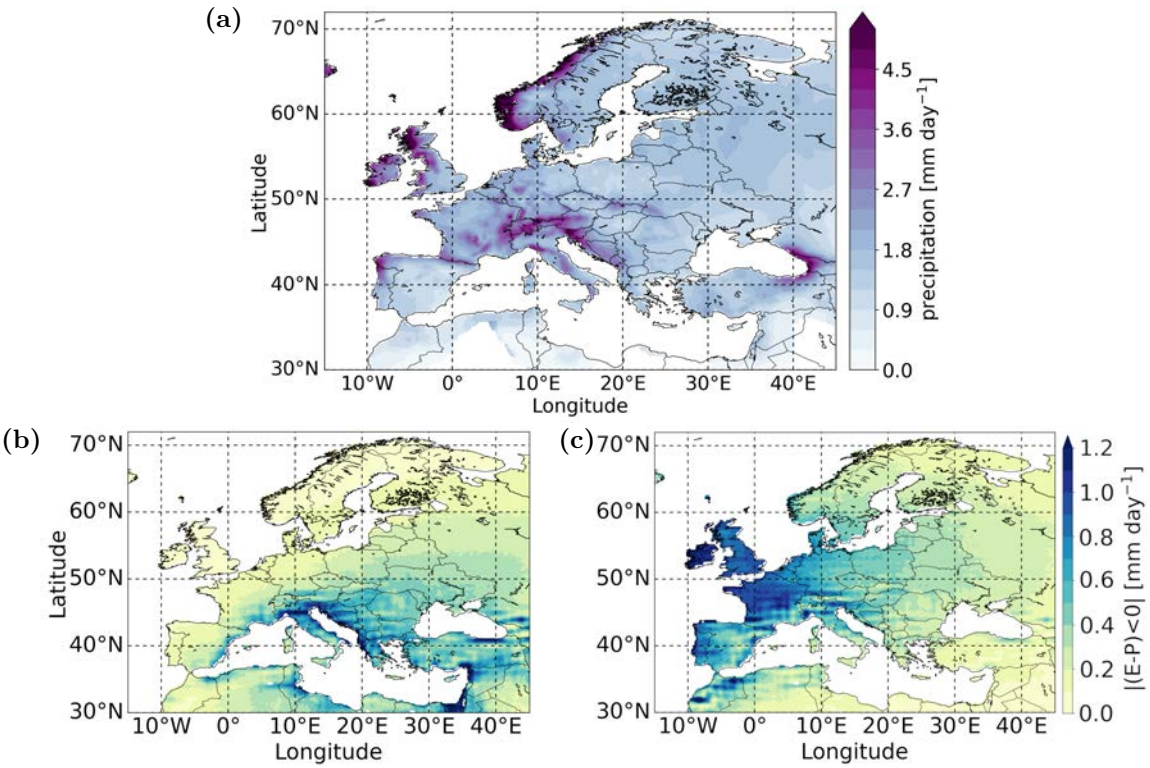

Figure 3.1: (a) Mean precipitation and mean moisture contribution to precipitation from the (b) MEDT and (c) NATL over Europe. Period 1980-2018. Note the different scales.

3.2 Linear relationship assessment over Europe

In a second analysis, the degree of linear relationship was assessed. Figure 3.2 shows the correlation between the WeMOi and the series of the precipitation (a) and the moisture contribution to precipitation ($|(E-P)<0|$) from the MEDT (b) and the NATL (c). The black line delimits the area that encloses statistically significant correlation values ($p < 0.05$).

The correlation values in figure 3.2a are positive and statistically significant over most of Europe. The highest positive correlations are found between the west coast of France and Eastern Germany, followed by those observed in Great Britain. In contrast, negative correlations prevail in the central and southern parts of the IP, which indicates that a negative phase of the WeMO, is related to the precipitation increase over this area.

In our literature search, we did not find any published and referenceable study that analysed the linear relationship of the WeMO with precipitation over Europe. However, previous findings computed and discussed the lagged bivariate correlation between the daily extreme precipitation anomaly over Europe and the WeMOi (Tabari and Willems 2018). They found that the WeMO teleconnection is the main driver of summer EP over much of Europe, but also reported lagged effects of summer WeMO

characteristics in the following seasons, although with an almost reversed EP pattern.

The correlation between the moisture contribution to precipitation from the MEDT and the WeMOi, shown in figure 3.2b, displays a different pattern. Here, the western part of Europe is negatively correlated, while the eastern part is positively correlated. This indicates that during positive WeMO phases, the MEDT contributes more to the precipitation over the Balkans and Eastern Europe, whereas during negative WeMO phases, it contributes more to the precipitation over the IP and Western Europe due to the southeasterly wind flow direction, as shown in Martin-Vide and Lopez-Bustins (2006) and Lopez-Bustins et al. (2020).

The pattern from figure 3.2a is nearly repeated for the moisture contribution to the precipitation from the NATL, shown in figure 3.2c, visually. Central and Eastern Europe, the Italian Peninsula and the Balkans are positively correlated, and the central and southern part of the IP is negatively correlated. Although the magnitude of the correlation values, and the area that negative values occupy over Central and Southern IP, decreases concerning those obtained for precipitation. Previous studies have revealed that the North Atlantic Ocean directly influences precipitation over Central Europe through moisture transport (Gimeno et al. 2011; Batibeniz et al. 2020).

This confirms the strong influence of the WeMO in and around the Mediterranean region. The hypothesis that a positive WeMO phase is related to a positive moisture flux from the NATL over Central Europe and therefore favouring precipitation over Central Europe, is evaluated in more detail in the next sections.

3.3 Hydroclimate anomalies during WeMOi(+/−) phases over Europe

In this section, the anomalies of precipitation and the moisture contribution to precipitation from the MEDT and NATL during a positive and a negative WeMOi (WeMOi(+/−)) are presented. First, in section 3.3.1, the annual anomalies are displayed and compared with the Eulerian VIMF patterns. This is followed by a detailed comparison of the anomalies during the opposite seasons, winter and summer (section 3.3.2). It is thus possible to determine the different influences of the WeMO during the different seasons of the year.

3.3.1 Annual hydroclimate anomalies

Figure 3.3 represents the anomalies of the precipitation (a,b), the moisture contribution to precipitation from the MEDT (c,d) and the NATL (e,f) caused by the WeMO(+)

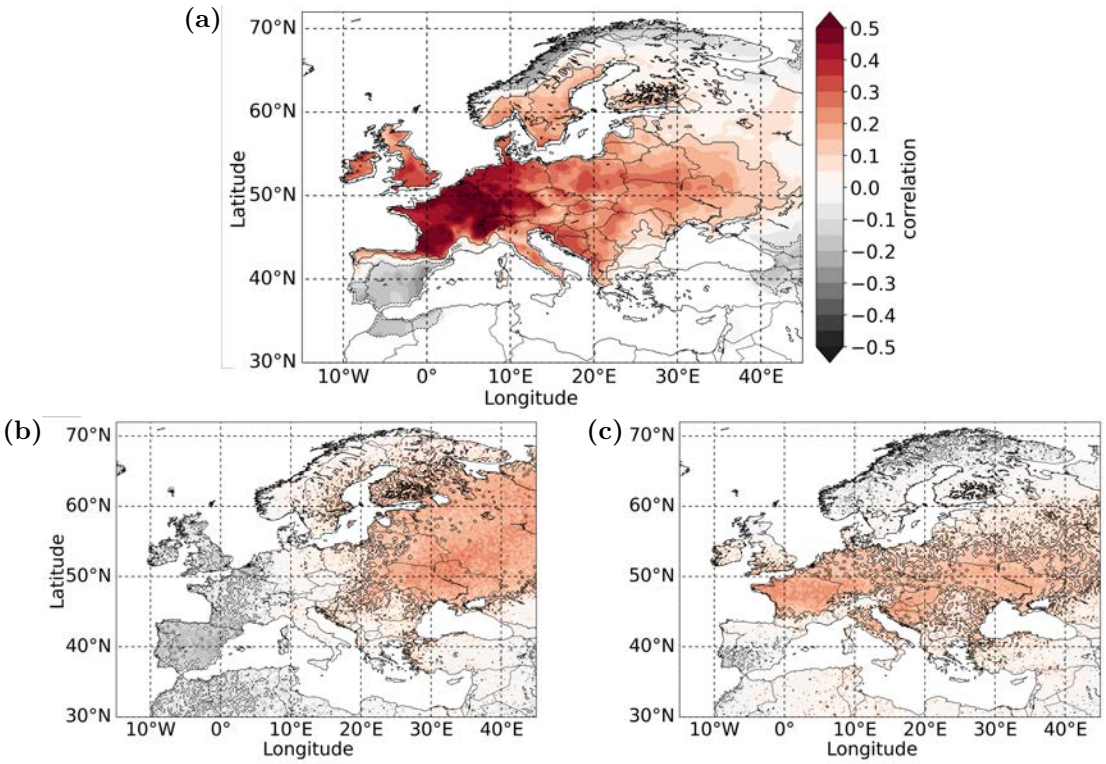

Figure 3.2: Correlation between (a) precipitation from E-OBS and the WeMOi, (b) the contribution to precipitation from the MEDT and the WeMOi and (c) the contribution to precipitation from the NATL and the WeMOi over Europe. Period: 1980-2018. Dashed/solid black lines indicate statistically significant values ($p < 0.05$).

and the WeMO(−) respectively. Under the influence of a WeMO(+), European areas between approximately 43°N and 60°N receive more precipitation than the climatological average while negative anomalies are observed almost everywhere in the IP, except for the northernmost region, where they are positive. This occurs in conjunction with the occurrence of negative anomalies of the moisture contribution from the MEDT over Western and part of Central Europe, especially in the Central and Southern IP, while positive anomaly values occupy part of Central and all of Eastern Europe. The pattern of anomalies of the moisture transport from the NATL also supports the pattern of the precipitation anomalies, with stronger positive moisture supply anomalies over France and the Balkans, and negative ones over the southeastern IP during a WeMOi(+).

Conversely, under the influence of a negative WeMO phase, the spatial pattern of the precipitation anomaly changes in the opposite direction. The central and southern parts of the IP and the Western Mediterranean coast receive more precipitation and Central Europe receives less. This is due to the increased moisture contributions to the precipitation over the former mentioned areas from the MEDT and the NATL, combined with the reduced moisture contributions to the precipitation over Western France and the Balkans from the NATL, and the reduced moisture contribution over the Balkans and Eastern Europe from the MEDT, as appreciated in figures 3.3d,f.

These patterns are consistent with the atmospheric flow directions forced by the WeMO and are presented for the first time in this study. Flow directions, in combination with the orography, place landmasses on the windward or leeward side of their moisture sources thereby inhibiting or allowing moisture transport and consequently the contribution to precipitation from these sources (Martinez-Artigas et al. 2021). During WeMO(+) phases, the atmospheric flow describes westerly/northwesterly directions in the western part of Europe and westerly/southwesterly directions in the eastern part of Europe. In contrast, during WeMO(−) phases, southeasterly directions can be observed in the western part of Europe and easterly/northeasterly directions in the eastern part of Europe (Martin-Vide and Lopez-Bustins 2006; Lopez-Bustins et al. 2020). This is confirmed by the anomalies of VIMF represented in figure 3.4.

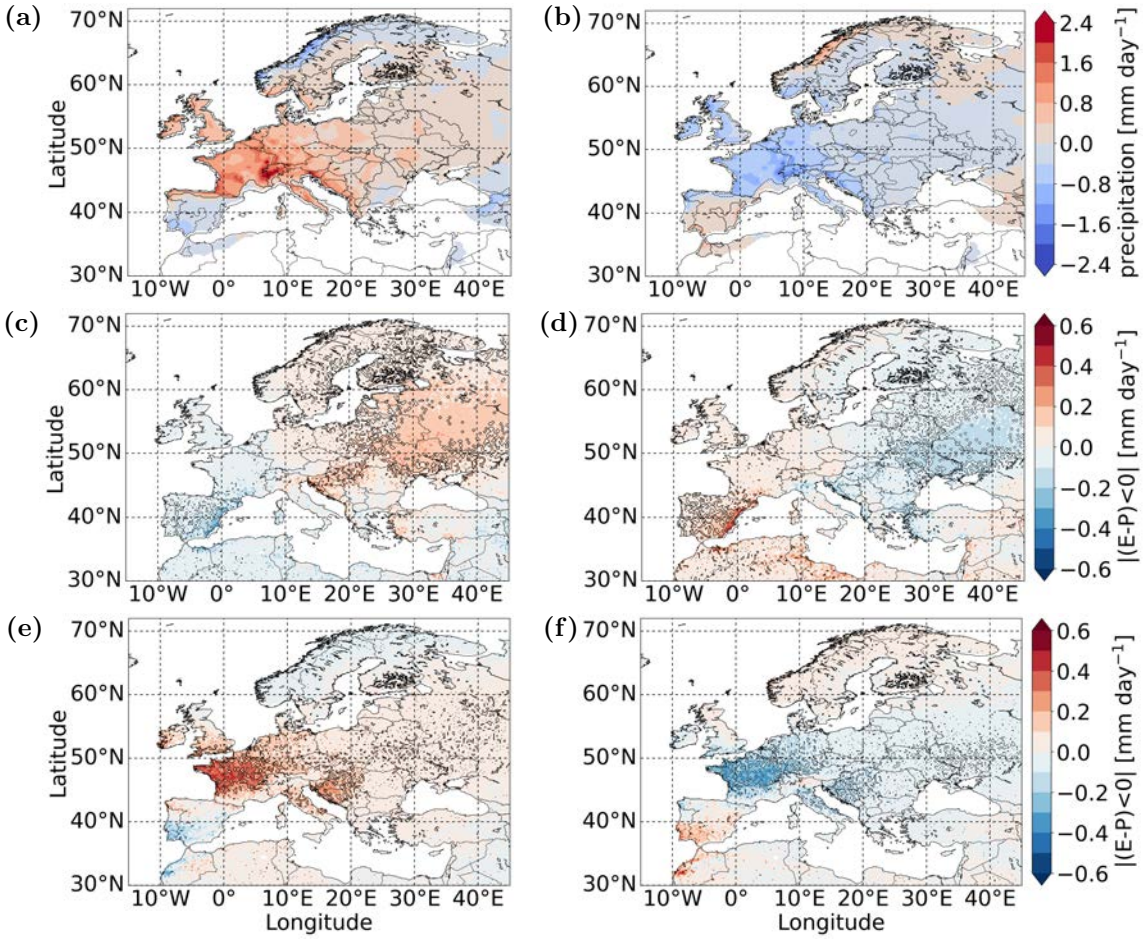

Figure 3.3: Anomalies of precipitation and the contributions to precipitation from the MEDT and NATL during a WeMOi(+/−). Period: 1980-2018. The left column represents anomalies during a WeMOi(+) and the right column represents anomalies during a WeMOi(−). (a,b) represent precipitation, (c,d) show the moisture contributions from the MEDT and (e,f) show the moisture contributions from the NATL. Dashed/solid black lines indicate statistically significant ($p < 0.05$) results, note the different scales.

As commented above, the VIMF anomalies and its divergence anomalies under a WeMOi(+/−) support the understanding of the Lagrangian moisture transport anomalies and the precipitation anomalies seen in figure 3.3. The VIMF convergence (warm colours) and divergence (cold colours) indicate areas where convective and precipitation processes are favoured and inhibited respectively.

During a WeMOi(+) (Fig. 3.4a), negative anomalies of the VIMF divergence over Central Europe, the Balkans and along the northern coast of the IP reveal the prevalence of convergence of the moisture flux and favouring the occurrence of precipitation. The anomalies in the circulation of the VIMF also reveal a cyclonic circulation with its centre located over Central Europe. Contrarily, VIMF divergence positive anomalies are observed over the Eastern NATL, the Central and Southern IP, and the Western MEDT. These are associated with an anticyclonic anomaly circulation of the VIMF, inhibiting precipitation, supporting the results described in figure 3.3.

During a WeMOi(−) (Fig. 3.4b), negative anomalies of the VIMF divergence indicate the prevalence of convergence over the Gulf of Cádiz and along the Mediterranean coast of the IP and France, combined with a cyclonic circulation anomaly. In addition, an increased VIMF divergence concerning climatology is observed over much of the rest of Europe, where an anticyclonic circulation anomaly of the VIMF can be observed. As already commented, these circulation anomalies are consistent with the expected WeMOi(+/−) atmospheric flow patterns (Martin-Vide and Lopez-Bustins 2006; Lopez-Bustins et al. 2020).

These results open up new questions, such as the role of the WeMO in the variability of the North Atlantic storm track, a mechanism that plays a crucial role in moisture transport and the European climate (Dong et al. 2013), and the occurrence of extreme precipitation, here assessed for the IP (section 3.4.4 and 3.4.5).

3.3.2 Seasonal hydroclimate anomalies

In this section, we evaluated the differences between seasonal anomalies of precipitation and $|(E - P) < 0|$ anomalies during a WeMOi(+/−), with a particular emphasis on the winter (DJF) and summer (JJA) seasons. The analysis for opposite climatic conditions allows us to avoid the signal of intra-annual climatic variations and to contrast the role of the WeMO during different climatic conditions of the year, which was not possible in section 3.3.1. Therefore, the winter and summer were chosen to deepen the analysis. Previous studies support this decision, according to Gómez-Hernández et al. (2013) and Batibeniz et al. (2020), the strongest effect on moisture transport from oceanic sources occurs over the IP and Europe during winter when teleconnections have the strongest influence (Martinez-Artigas et al. 2021).

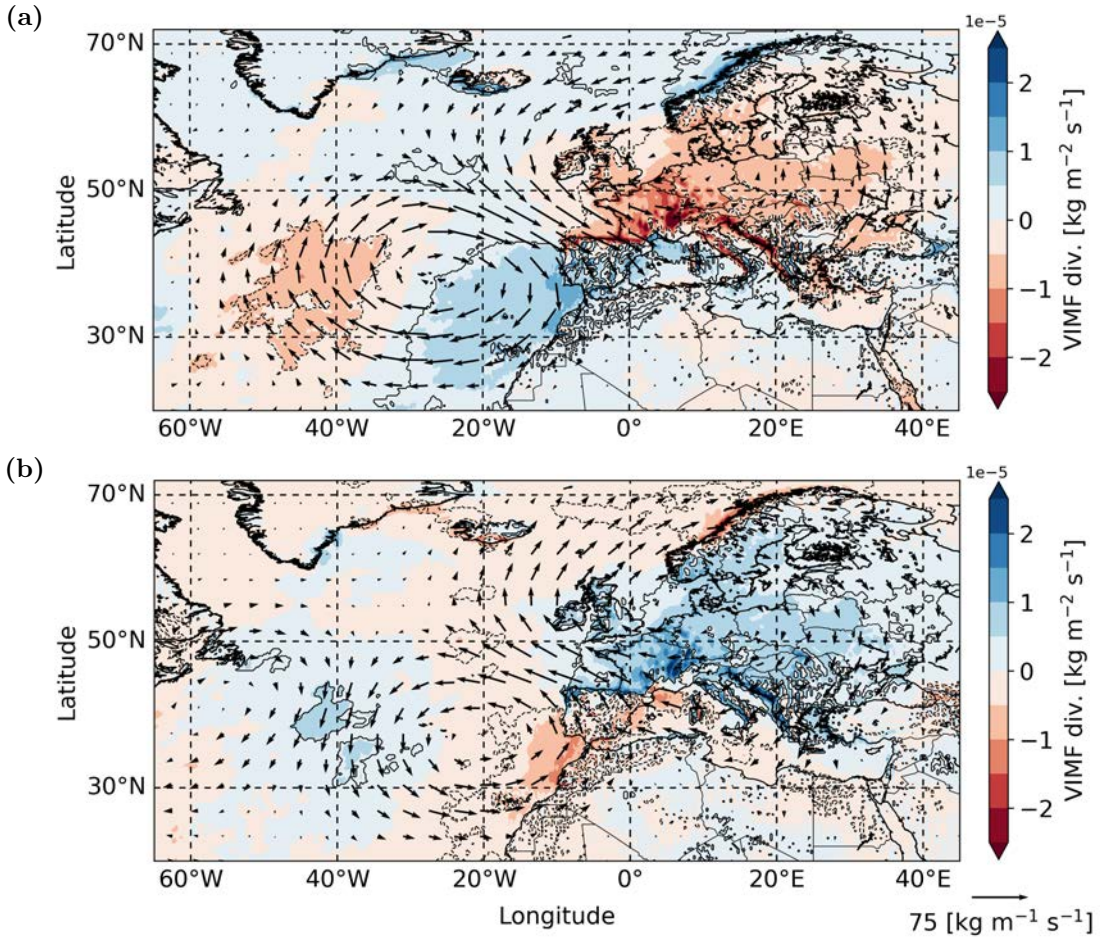

Figure 3.4: Anomalies of the VIMF during a WeMOi(+/−).Period: 1980-2018. (a) represents anomalies during a WeMOi(+) and (b) represents anomalies during a WeMOi(−). Dashed/solid black lines indicate statistically significant ($p < 0.05$) VIMF divergence anomalies, arrows indicate VIWVF anomalies.

Conversely, we consider summer as the season with the lowest precipitation rate over the IP (Shahi et al. 2022). In addition, the WeMO was found to play a role in the occurrence of extreme precipitation events over Europe during the summer (Tabari and Willems 2018).

From a visual analysis of the precipitation anomalies under the WeMO(+/−) for DJF and JJA (Fig. 3.5), the following can be summarised. For winter under a WeMOi(+) (Fig. 3.5a), positive precipitation anomalies are observed over Central and Eastern Europe, but negative anomalies are found over the Western Mediterranean region, including most of the IP, except for its northern region. On the contrary, under the influence of the negative phase of the WeMO during winter (Fig. 3.5b), this pattern of anomalies is reversed, with more precipitation than usual over the Western Mediterranean, particularly over the southwestern IP. This is consistent with the annual analysis shown in figures 3.3a,b.

For the summer (Fig. 3.5c,d), the pattern of anomalies is somewhat similar to the winter season. However, under WeMO(+/−) conditions, the strongest positive and negative anomalies appear more towards central-eastern Europe compared to the pattern observed for winter. In addition, the magnitude of the anomalies is more pronounced for DJF than for JJA. Over the Central and Southern IP, there is nearly no response to the different WeMO(+/−) phases, which goes along with Martinez-Artigas et al. (2021), who found the weakest relationships during summer between the WeMO and the precipitation over this region.

The precipitation anomaly patterns for autumn and spring (Fig. S3.1) are consistent with the annual ones (Fig. 3.3a,b). Compared to winter, the positive anomalies observed for autumn (Fig. S3.1a,b) are stronger under the influence of a WeMO(+), but weaker under a WeMO(−). However, the statistically significant positive anomaly area of the precipitation under a WeMOi(−) over the southeastern IP is larger than in the rest of the season. This is coherent with Martin-Vide and Lopez-Bustins (2006) and Lopez-Bustins and Lemus-Canovas (2020), as they confirmed a strong relationship between the precipitation in the southeastern IP and negative WeMO conditions during autumn. For the spring season, a similar effect of the WeMO on the signs of the precipitation anomalies was found, they were weaker than during winter and autumn, but stronger than during summer over Central Europe.

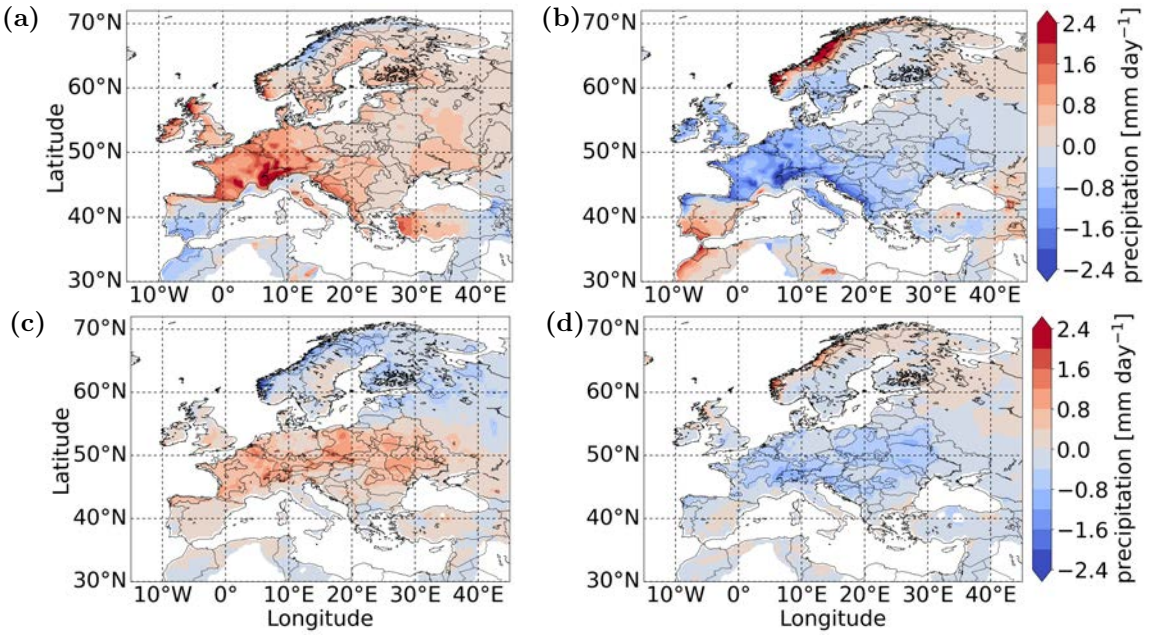

Figure 3.5: Anomalies in precipitation during DJF (top) and JJA (bottom) under the influence of positive (left column) and negative (right column) WeMOi phases. Period: 1980-2018. Dashed/solid black lines delimit areas with statistically significant ($p < 0.05$) values.

The seasonal anomalies on the moisture contribution from the MEDT and NATL sources under the influence of the WeMO(+/−) were also determined, and are plotted

for summer and winter in figure 3.6, and for autumn and spring in figure S3.2. The anomalies of $|(E-P) < 0|$ from the MEDT for DJF are characterised by positive (negative) values over eastern and southeastern Europe under the positive (negative) phase of the WeMO. Opposite patterns were found over the Western Mediterranean coast (Fig. 3.6a,b). In contrast to the annual analysis of the IP, the anomalies are more concentrated along the coast, confirming the importance of showing seasonal differences. During the same season, the anomalies in the moisture contributions to precipitation from the NATL under a WeMOi(+) reflect stronger positive anomalies across the major part of western-central to Eastern Europe, including the northwestern IP, Great Britain and the Balkans. Negative anomalies are enclosed over the southeastern IP (Fig. 3.6c). The opposite pattern is observed under a WeMOi(−) (Fig. 3.6d).

In summer, the anomalies in $|(E-P) < 0|$ from the MEDT over Eastern Europe are weaker than in winter, while the anomalies over the IP remain similar (Fig. 3.6e,f). Batibeniz et al. (2020) also found stronger intra-annual changes in moisture transport from the MEDT over Eastern Europe, although they did not relate these changes to the WeMO. For the moisture contribution anomalies from the NATL in JJA, we observed positive anomalies over Western France and the Balkans during a WeMOi(+) and positive anomalies over the central and southern part of the IP during a WeMOi(−) (Fig. 3.6g,h). The anomalies are weaker in summer than in winter.

Figure S3.2 shows that during autumn and spring, the anomaly patterns from both sources are very similar to those already described for winter and summer. However, in autumn, the anomalies over the southeastern IP are stronger than in winter. Finally, for the anomalies in the moisture contribution to precipitation from the NATL, it appears that the pattern is shifted northward during winter compared to autumn and spring. These results evidence that for both WeMO phases the spatial patterns of $|(E-P) < 0|$ are very similar concerning the annual results (Fig. 3.3c-f)

The stronger variability during the boreal winter can be explained by a generally stronger moisture advection from oceanic sources, which is more influenced by teleconnection processes (Martinez-Artigas et al. 2021), while during boreal summer the recycling becomes stronger (Gómez-Hernández et al. 2013; Batibeniz et al. 2020; and see section 3.4.2). Particularly, for the NATL, a stronger impact of the moisture advection to Europe during the winter months was reported (Gimeno et al. 2010b; Castillo et al. 2014; Batibeniz et al. 2020). Additionally, the moisture transport from oceanic sources is strongly influenced by evaporation and horizontal winds, which are higher in winter than in summer over the NATL (Walsh and Portis 1999) and the MEDT (Mariotti et al. 2002; Sánchez Gómez et al. 2009; Zveryaev and Hannachi 2022). Thus, stronger winds in combination with less moisture content during winter can lead to increased evaporation (Zveryaev and Hannachi 2022). Furthermore,

former studies pointed out that the WeMOi represents precipitation better in the boreal winter months (Martin-Vide and Lopez-Bustins 2006; Lopez-Bustins and Lemus-Canovas 2020; Martinez-Artigas et al. 2021).

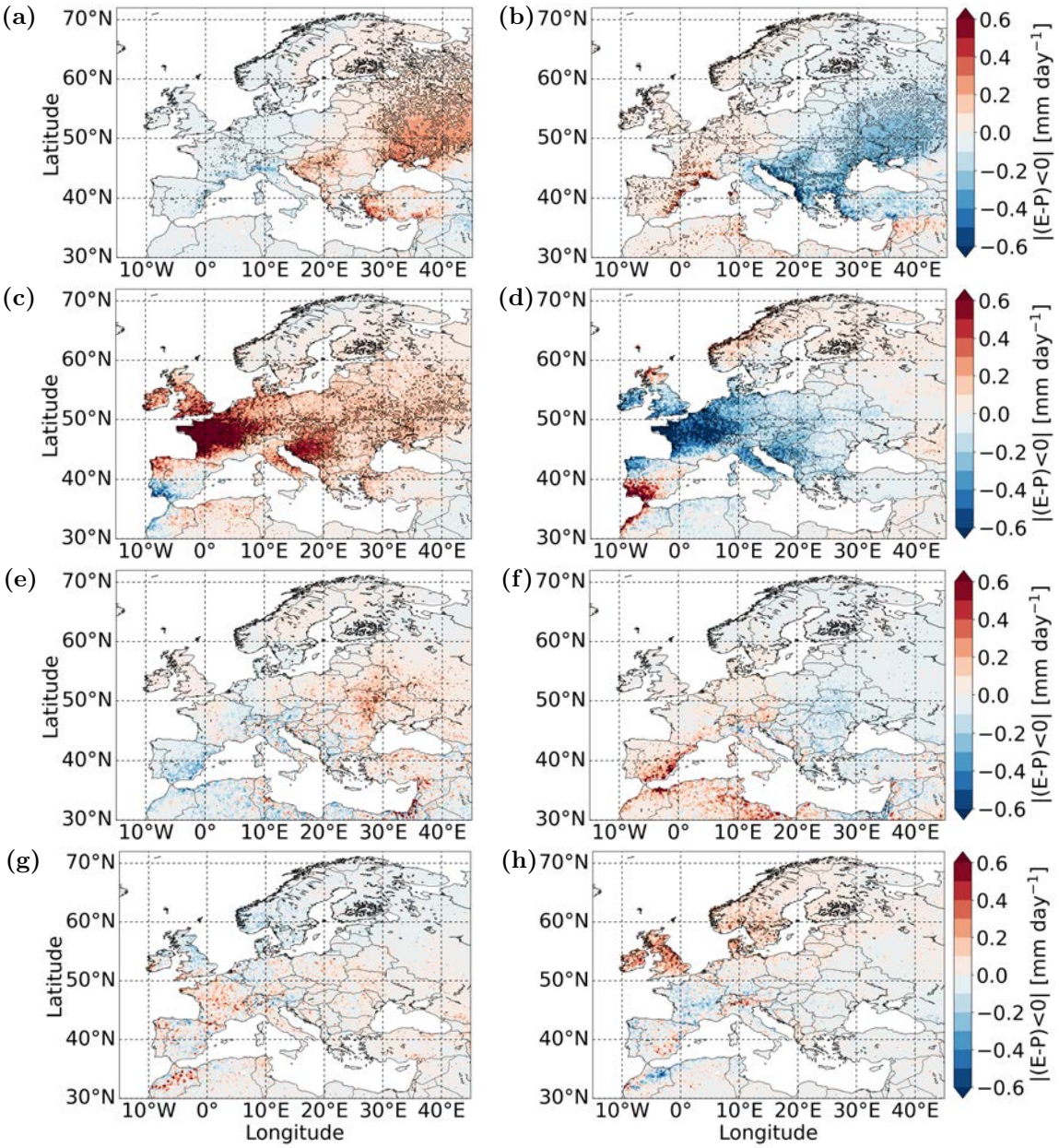

Figure 3.6: Anomalies of the moisture contribution to precipitation from the MEDT and NATL during a WeMOi(+/−). Period: 1980-2018. The left column represents anomalies during a WeMOi(+) and the right column represents anomalies during a WeMOi(−). (a,b) represent the DJF anomalies on the contribution from the MEDT and (c,d) from the NATL. (e,f) represent the JJA anomalies on the contribution from the MEDT and (g,h) from the NATL. Dashed/solid black lines indicate statistically significant ($p < 0.05$) values.

The anomalies of the VIMF and its divergence (Fig. 3.7) are consistent with the Lagrangian $|(E - P) < 0|$ results represented in figure 3.6. In winter (Fig. 3.7a,b),

the magnitude of the VIMF divergence and circulation anomalies is higher than in summer and in the annual analysis (Fig. 3.4), but a similar pattern is shown. In this season, under the influence of a WeMO(+), positive VIMF divergence anomalies are observed over the Eastern NATL and the Western Mediterranean, including its coast. As in the annual analysis, an anticyclonic circulation anomaly, with its centre over the Azores is found. In addition, Negative VIMF divergence anomalies are observed over the Northern IP coast, western-central Europe, the Balkans and Greece, indicating more convergence. This is associated with a cyclonic circulation anomaly of the VIMF from Great Britain to Eastern Europe, passing the Northern MEDT and Central Europe. Thus, VIMF vectors can be observed from the northwest over Western Europe and the southwest over Eastern Europe, indicating the moisture transport observed in figure 3.6. Conversely, with a negative WeMOi, opposite spatial anomalies are obtained.

Previous studies have confirmed the importance of the WeMO and other teleconnection modes, such as the North Atlantic Oscillation (NAO) and the Arctic Oscillation (AO), for the understanding of precipitation variability and trends at regional scales like the IP (Lopez-Bustins et al. 2008) or the European Mediterranean region (Seager et al. 2020) during winter. This is caused by changes in atmospheric circulation. As for the annual analysis, the VIMF vectors indicate the moisture flow as thought by other studies (Martin-Vide and Lopez-Bustins 2006; Lopez-Bustins and Lemus-Canovas 2020; Martinez-Artigas et al. 2021) over the IP during WeMO(+/−) phases.

In summer, during WeMOi(+) phases, slightly positive VIMF divergence anomalies are found over the central and southern IP and the Western Mediterranean coast. Negative anomalies are found over Central and Eastern Europe, the Balkans and Greece, with a minimum over Eastern Europe, and a cyclonic VIMF circulation over Europe. Again, opposite anomalies result during a WeMOi(−), with a VIMF divergence anomaly maximum northeast of the Balkans. An anticyclonic circulation of the VIMF was found over Europe.

The VIMF divergence anomaly patterns for autumn under the WeMOi(+/−) are very similar to the pattern for winter (Fig. S3.3a,b). Autumn and spring present weaker anomalies of VIMF than during winter, but stronger than during summer. The magnitude of the winter and autumn anomaly patterns plays a determining role in the coincidence observed with the annual patterns seen in figure 3.4.

3.4 The Iberian Peninsula hydroclimate and the WeMO

As mentioned in the introduction and documented in section 3.3, the WeMO is an important mode of climate variability for the Iberian hydroclimate. Furthermore, it has

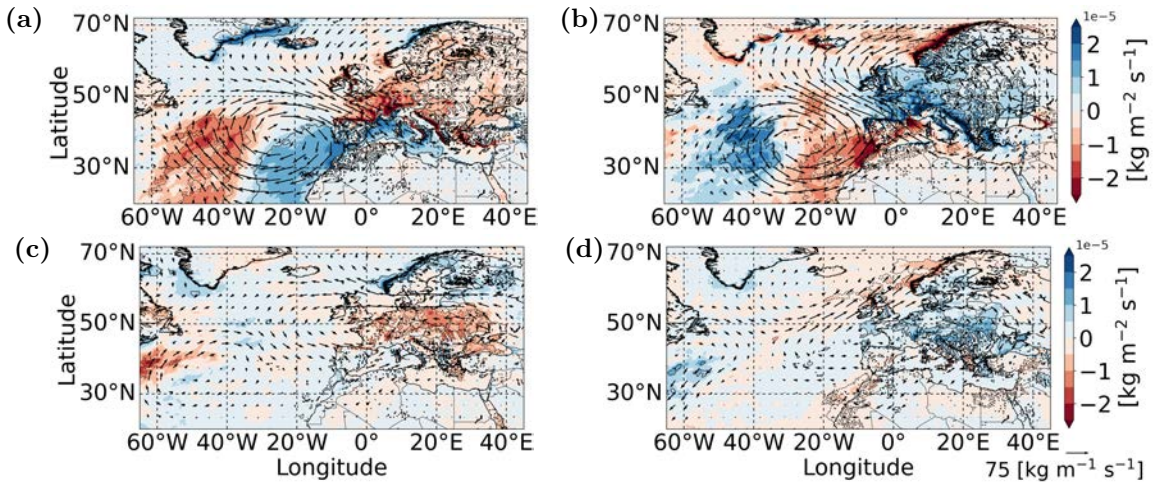

Figure 3.7: Anomalies of the VIMF during DJF (top) and JJA (bottom) under the influence of positive (left column) and negative (right column) WeMOi phases. Period: 1980-2018. Dashed/solid black lines delimit VIMF divergence areas with statistically significant ($p < 0.05$) values, arrows indicate VIMF anomalies.

been seen that the IP is one of the regions most influenced by the WeMO. Therefore, an analysis of precipitation patterns, and especially extreme precipitation patterns, under different WeMO conditions has been carried out specifically for this region. The following analysis was done for the period 1980-2015, taking into account the availability of data in Iberia01.

3.4.1 The linear relationship distinguishes two zones

Two latitudinally differentiated zones within the IP have been defined, according to opposite statistically significant ($p < 0.05$) correlation values between the precipitation from the Iberia01 dataset and the WeMOi (Fig. 3.8a). An area of positive correlation was found in the northern part of the IP and an area of negative correlation was found covering a central-southern region. To better visualise the northern and south-central zones, which will be used in the following analyses, a schematic figure was drawn up and is shown in figure 3.8b. The northern zone of the IP experiences positive anomalies of precipitation during positive WeMO phases, while in the central-southern zone, it is reversed. As section 3.3 demonstrated, during a WeMOi(+), the northern IP receives more moisture from the NATL, and during a WeMOi(−), the southwestern IP receives more moisture from the NATL and the southeastern IP receives more moisture from the MEDT.

The same results obtained through two different datasets confirm the spatial response of the precipitation over the IP to the influence of the WeMO. This can be explained by the complex topography of the IP and the flow patterns described by Martin-Vide and Lopez-Bustins (2006) and Martinez-Artigas et al. (2021), confirming

not only the local (Lopez-Bustins and Lemus-Canovas 2020; Benetó and Khodayar 2023) but also the regional (Martin-Vide and Lopez-Bustins 2006; Merino et al. 2016; Martinez-Artigas et al. 2021) character of the WeMO in the modulation of the IP hydroclimate. Similar correlation patterns were found by Martin-Vide and Lopez-Bustins (2006) and Martinez-Artigas et al. (2021).

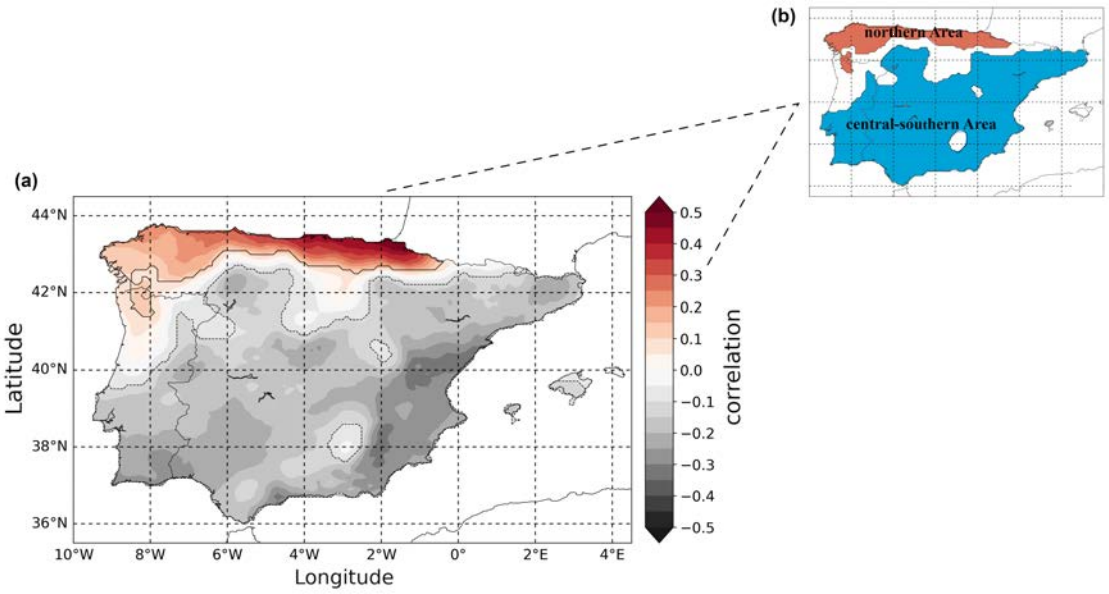

Figure 3.8: (a) Correlation between the precipitation from Iberia01 and the WeMOi over the IP. Period: 1980-2015. Dashed/solid lines indicate significant results ($p < 0.05$). (b) Schematic representation of the northern and central-southern zones.

3.4.2 Moisture origin and the WeMO

As already mentioned, various studies have pointed out that the MEDT and NATL are important sources of moisture for the precipitation over the IP. In addition, we considered that precipitation from terrestrial origin could play an important role, and therefore considered the IP as a source of moisture for itself. To assess it, daily data of $|(E - P) < 0|$ computed over the northern and central-southern zones from a FLEXPART forward in time analysis from each source were used.

Figure 3.9 shows the seasonal average contribution (in percentage) from each source for the northern and central-southern zones. This analysis reveals that for the four seasons, the NATL was responsible for supplying the greater amount of moisture for the precipitation ($\geq 84\%$) in the northern zone, followed by the MEDT and the IP (Fig. 3.9a). These findings are very similar for the central-southern zone (Fig. 3.9b), although the MEDT and the IP slightly increase their contribution while that from NATL decreases, but remains above 79% of the total. Thus, the MEDT and IP gain importance concerning the NATL when going from the northern zone to the central-

southern one. Furthermore, the MEDT plays a stronger importance during winter and autumn, as the WeMO(−) which favours more a southeasterly flow (Martin-Vide and Lopez-Bustins 2006; Martinez-Artigas et al. 2021). In addition, the moisture contribution from the IP itself with respect to the other sources increases from winter to autumn for the central-southern zone, and it is strongest in autumn over both zones.

It should be noted that figure 3.9 represents the distribution of $|(E-P)<0|$ from the three selected moisture sources concerning their total contribution. Thus, higher percentage values do not mean that the absolute contributions (e.g. terrestrial) are higher during one season than during others. Indeed, for both zones, the greatest contribution from the terrestrial contribution occurs during the summer ($1.5e^{-3}$ mm day^{-1} and $2.7e^{-3}$ mm day^{-1} in the northern and central-southern zone respectively). This contribution may be considered moisture recycling, which is defined as the moisture that contributes to precipitation evaporating from the area where it precipitates. Gómez-Hernández et al. (2013) and Rios-Entenza et al. (2014) also found stronger recycling importance for the IP during the dry season than during the wet season and during summer than during winter. Additionally, Batibeniz et al. (2020) found the strongest recycling influence during late spring and summer.

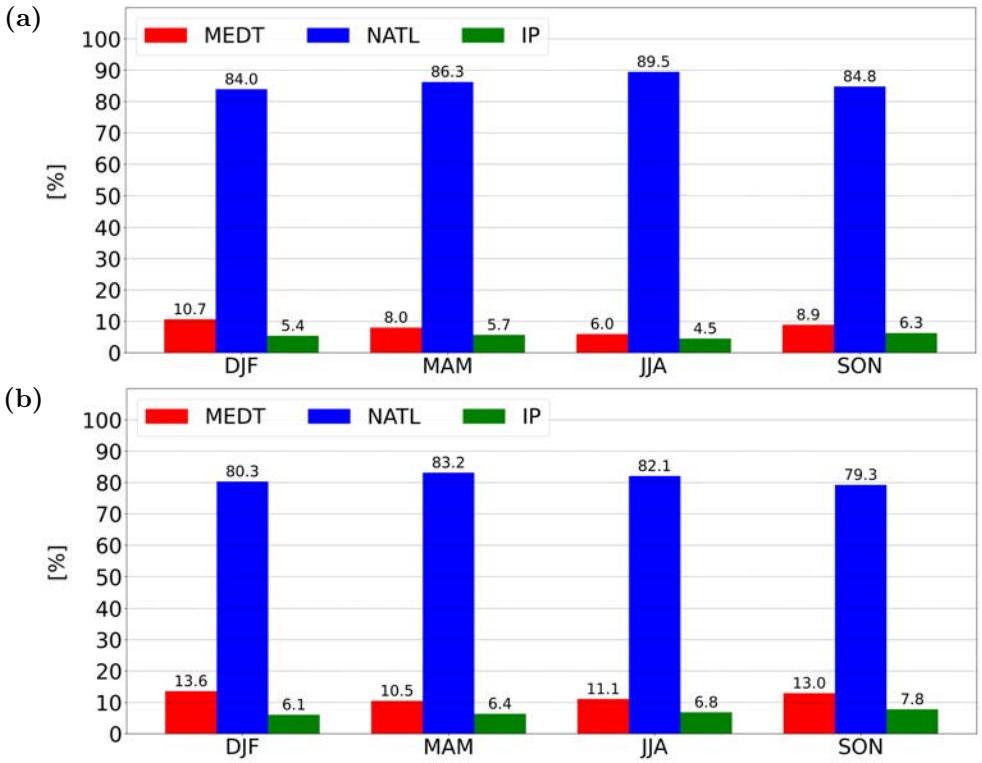

Figure 3.9: The mean moisture contributions to precipitation (in percentage) from the MEDT (red), the NATL (blue) and the IP (green) to the IP. Period: 1980-2015. For winter (DJF), spring (MAM), summer (JJA) and autumn (SON) averaged over the (a) northern zone and (b) central-southern zone.

3.4.3 Temporal evolution: Hydroclimate and the WeMO

Several recent studies (e.g. Pereira et al. 2021; Insua-Costa et al. 2022; Senent-Aparicio et al. 2023) analysed the temporal evolution of the precipitation and moisture transport over Spain and the IP. In this work, we also have this objective, but taking into account the spatial differentiation (northern and central-southern zones) that occurs in precipitation over the IP in response to positive and negative WeMO conditions. A temporal evolution of the annual mean values of the WeMOi, the precipitation, and the moisture contribution from the MEDT and NATL sources, from 1980 to 2015 was performed. These are shown alongside the linear trends of each series in figures 3.10a,b, for the northern and central-southern zones respectively.

The temporal evolution of the WeMOi does not reveal the existence of any cyclicality between the negative and positive phases but experienced a statistically significant negative trend ($-2.15e^{-2}$ year^{-1}). This negative trend coincides with a slightly negative, although statistically non-significant, trend in precipitation values over the northern zone of the IP. In addition, there is a statistically non-significant negative trend in the moisture contribution to the precipitation from the MEDT and a positive and statistically significant trend in the contribution to the precipitation from the NATL over this zone (Fig. 3.10a). Conversely, figure 3.10b reveals a positive trend, (not statistically significant) in the precipitation over the central-southern zone of the IP, accompanied by a positive trend in the moisture contribution to the precipitation from the MEDT and the NATL.

Our results are in agreement with various studies. Martin-Vide and Lopez-Bustins (2006) already described a negative WeMOi trend for the latest half of the 20th century. Moreover, they also found a significant positive precipitation trend at a station in Valencia (central-southern zone) and a significant negative precipitation trend at a station in Bilbao (northern zone) during winter (October to March) for the period 1910-2000. Furthermore, Lopez-Bustins et al. (2008) explained, a precipitation decrease in the Bay of Biscay due to a decrease in the WeMOi, as in this region the WeMOi and the precipitation are positively correlated. Pereira et al. (2021) concluded that precipitation generally decreased from 1950 to the first decades of the 21st century over the IP, but the extreme precipitation increased. A regionalised study by Senent-Aparicio et al. (2023) noted a significant annual precipitation decrease over parts of Eastern, Southern and Central Spain and a significant increase over parts of Galicia and Asturias from 1951 to 2019. These results differ from ours and others cited above, which may be because these authors calculated the precipitation trend averaged over the whole of Spain (Pereira et al. 2021), or over each grid point (Senent-Aparicio et al. 2023), and even for a different period.

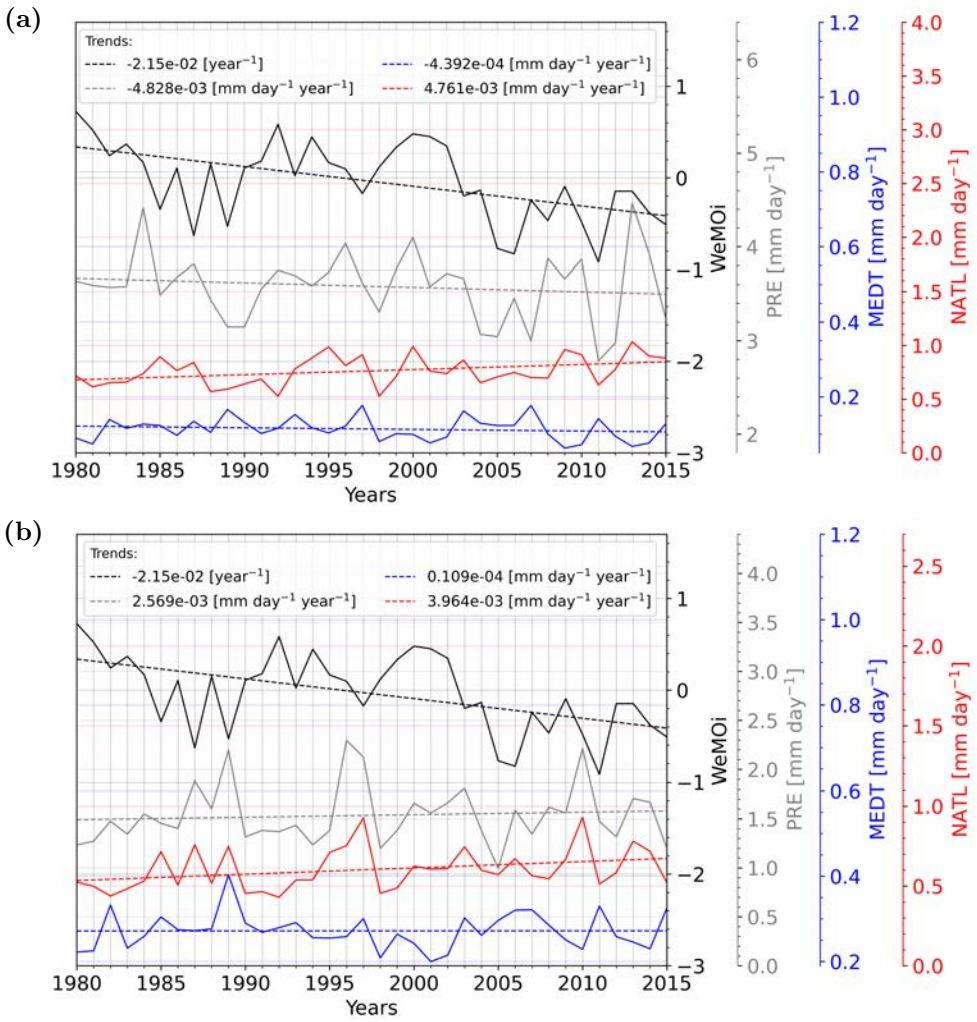

Figure 3.10: Temporal evolution of annual mean values of the WeMOi (black), precipitation (grey), and the moisture contribution to precipitation from the MEDT (blue) and the NATL (red). Period: 1980-2015. Dashed lines show the trend line with the slope number in the legend. (a) Represents the northern zone of the IP and (b) represents the central-southern zone of the IP, note the different scales.

The spatial representation of the precipitation and moisture contribution trend from figure 3.11 provides more information about the role of each source of moisture during the study period. We found the strongest negative precipitation trends over the northwestern IP and the Bay of Biscay, and the strongest positive precipitation trends over the coast of Asturias and northeastern Portugal (Fig. 3.11a). Weaker negative trends were found over the southern coast of Portugal, the Central IP, the southwestern Pyrenees and much of Cataluña. In addition, there are positive trends along the coast from Lisbon to Southern Galicia, the Southern IP, the southeastern Pyrenees and over large parts of the central-southern zone. The trend patterns of Senent-Aparicio et al. (2023) are somewhat consistent with our results, although differ concerning the significant areas and Galicia.

Visually, it can be summarized that the overall moisture contribution to precipitation from the MEDT increased less than from the NATL. Figure 3.11b describes slightly and mostly non-significant positive trends in the moisture contribution from the MEDT along the Mediterranean coast of the IP. Figure 3.11c shows stronger positive trends in the moisture contribution from the NATL, with maxima in the eastern and northwestern coasts and the southwestern area of the IP. The positive precipitation trends over the Southern IP are consistent with the increase in moisture contributions from the MEDT and NATL over this area. It should be noted that the precipitation trends over the IP do not always have to coincide with the trend of the contribution from the NATL and the MEDT, as seen in figure 3.10a. A better comparison of trends would be made by comparing the precipitation trend and the total moisture contribution from oceanic and terrestrial sources.

Furthermore, WeMO(+) phases lead to more precipitation over the northern IP and WeMO(−) phases lead to more precipitation over the central-southern IP, as seen in figure 3.8a. Thus, a negative WeMOi trend is associated with less precipitation in the north and more precipitation in the south. Moreover, during the WeMO(−) phases, the southwestern IP receives more moisture from the NATL and the Mediterranean coast of the IP receives more from the MEDT compared to other periods. Therefore, the positive trends of figures 3.11b,c over these regions are consistent with a WeMOi(−) trend of figure 3.10. Insua-Costa et al. (2022) performed a trend analysis for moisture transport from the MEDT and NATL for each season, and their observations can be explained by a decreasing WeMOi.

3.4.4 Extreme precipitation

Former studies have shown that overall precipitation patterns have decreased in recent years, while the trend of extreme precipitation (EP) has increased over the IP (Pereira et al. 2021; Senent-Aparicio et al. 2023). Additionally, the WeMO has been linked to EP over the Iberian Peninsula (Merino et al. 2016; Lopez-Bustins et al. 2020). This section analyses the relationship between daily EP and different WeMO phases. In more detail, this assessment focuses on the number of days with EP and the area occupied by EP in the northern and central-southern zones during positive (WeMOi ≥ 1), negative (WeMOi ≤ 1) and neutral ($-1 <$WeMOi< 1) WeMO conditions.

Figure 3.12 shows the number of days with EP over the IP, expressed in percentage, during months under a WeMOi(+) and a WeMOi(−), concerning the total number of days with EP. It was found that during a WeMOi(+), the northern zone of the Iberian Peninsula is more affected by EP, in particular, the coastal part of the Bay of Biscay (Fig. 3.12a). In contrast, during a WeMOi(−), the central-southern

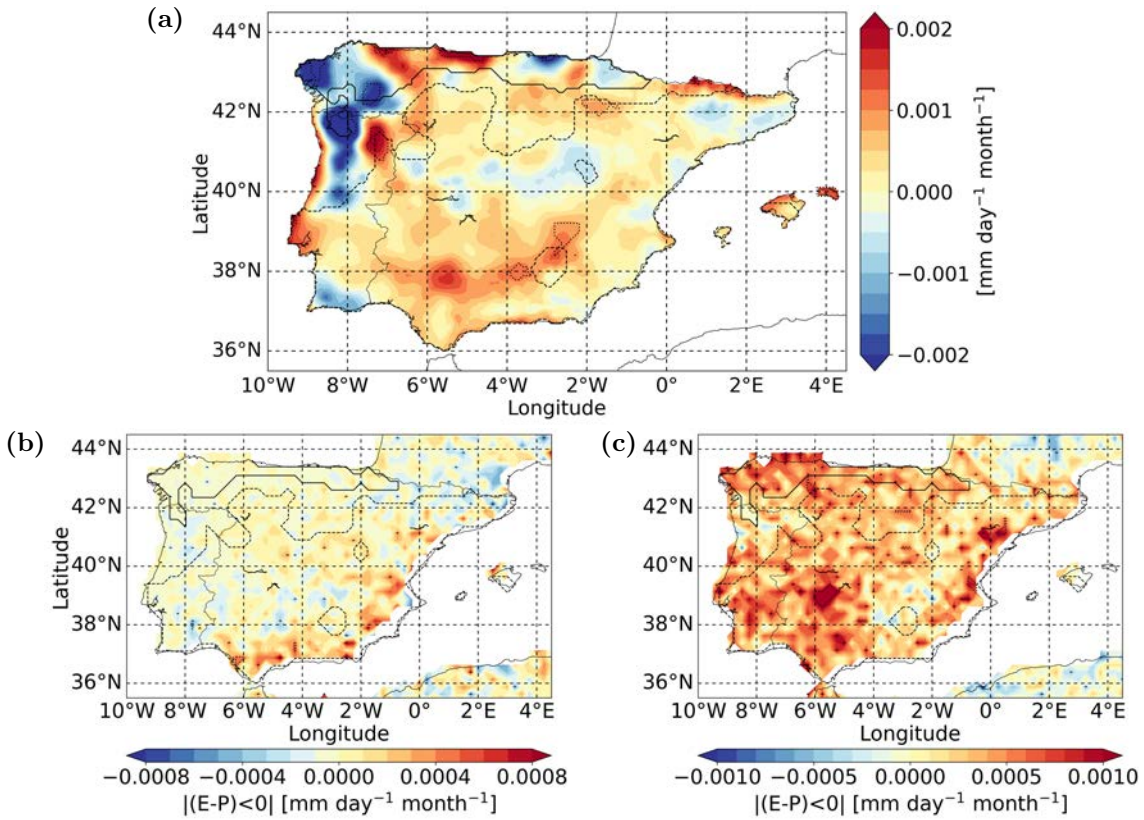

Figure 3.11: Monthly trend of (a) precipitation, and the moisture contribution to precipitation from the (b) MEDT and the (c) NATL. Period: 1980-2015. Solid/dashed lines indicate the northern/central-southern zone and pointed lines indicate statistically significant trends, note the different scales.

zone is more affected by days with EP, particularly the Mediterranean coast and the southwestern part of the peninsula (Fig. 3.12b). This observation is consistent with the pattern found by Merino et al. (2016), except for Galicia, as well as with the positive correlation between the precipitation and the WeMOi in the northern zone and a negative correlation in the central-southern zone, as seen in figure 3.8a. Furthermore, Lopez-Bustins et al. (2020) also found an increase in the number of torrential precipitation events during WeMOi(−) periods in Eastern Spain.

The monthly distribution of the average number of days with EP during WeMOi(+/−/0) phases, indicates that the northern zone is more affected under a WeMOi(+), while the central-southern zone is more affected under a WeMOi(−), which is supported by Merino et al. (2016). Over the northern zone, the number of EP events peaks during the late autumn and early winter months in comparison with other seasons, as can be seen in figure 3.13a. This finding is supported by Cardoso Pereira et al. (2020), who also observed a higher number of EP events during winter than during other seasons in the northern IP.

In the central-southern zone, the season cycle is not as simple as for the

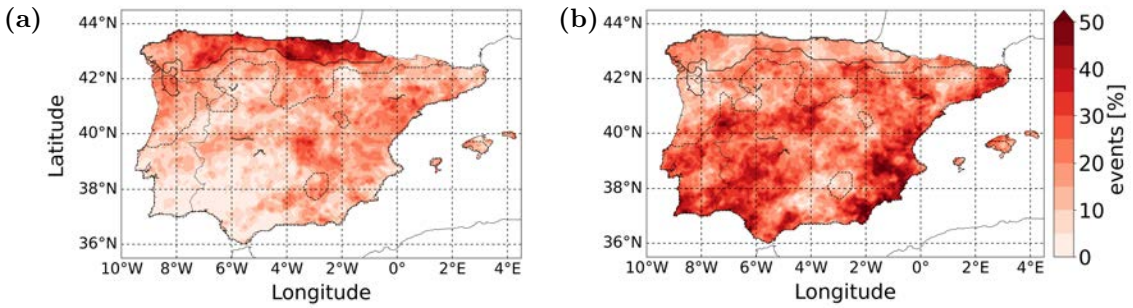

Figure 3.12: Percentage of days with EP (those with precipitation exceeding the 99th percentile) during (a) WeMOi(+) and (b) WeMOi(−) phases, with respect to the total number of EP days over the IP for each grid cell. Period: 1980-2015. Solid/dashed lines indicate the northern/central-southern zone.

northern IP. Figure 3.13b shows a main peak in late autumn and early winter (November-December) and a secondary peak in late spring (May) of EP events during a WeMOi(−). This can be attributed to the commonly torrential rainfall events during spring and autumn in the Eastern IP (Martin-Vide and Lopez-Bustins 2006; Lopez-Bustins et al. 2020; Cardoso Pereira et al. 2020), where the WeMO plays a major role (Martin-Vide and Lopez-Bustins 2006; Lopez-Bustins et al. 2020). The main peak of EP events under WeMOi(+/0) conditions is slightly earlier (October) than under a WeMOi(−). Differences in the number of EP days between WeMOi(+) and WeMOi(−) conditions are more pronounced in the central-southern zone and in winter. This can be explained by a generally stronger influence of the WeMO(−) in this zone, particularly during winter (Martin-Vide and Lopez-Bustins 2006; Lopez-Bustins et al. 2008; Lopez-Bustins and Lemus-Canovas 2020).

The monthly distribution of the mean area (in percentage) occupied by EP over the northern and central-southern zones (Fig. 3.14), was also determined. For the northern zone (Fig. 3.14a) the average area occupied by EP during a WeMOi(−) is slightly greater than during a WeMO(+/0). In addition, from the beginning of the rainy season (September) to the last month of the year, the major average area occupied by EP occurred under the influence of a WeMOi(−). This result does not seem to agree very well with that described in figure 3.13a, which observes more EP events under WeMOi(+) in the northern zone all year. Therefore, it can be suggested that the events under the influence of a WeMO(−), although fewer in number, occupy on average a larger area. However, it may also be conditioned by the calculation process. Since we used daily precipitation data and the monthly WeMOi, we categorised EP according to the different WeMO phases based on the months they occurred. Subsequently, an arithmetic mean was calculated for each month and the different WeMO categories, influenced by the number of events and the area occupied by each one.

Despite this, the monthly evolution of the occupied area under the three WeMO

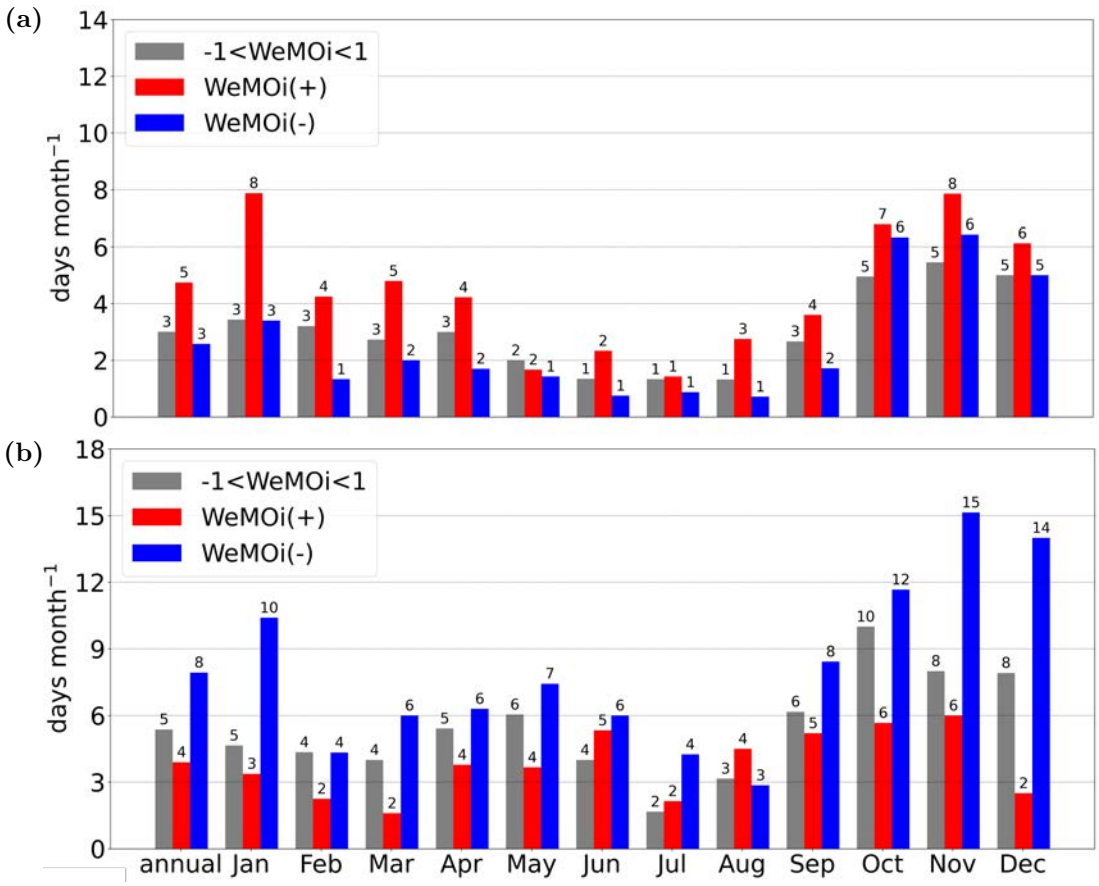

Figure 3.13: Average number of days with EP per month during the WeMOi(+/−/0) in the (a) northern zone and (b) central-southern zone. Period: 1980-2015. Note the different scales.

categories roughly represents the seasonal cycle of the EP days illustrated in figure 3.13a. However, a stronger difference between the mean areas during the WeMOi(+) and WeMOi(−) was found in the summer (July-August), when the highest mean areas of EP were observed for the WeMOi(+) phases (Fig. 3.14a). This is explained by the stronger influence of the WeMO(+) over this area and during summer, while the influence of the WeMO(−) is weaker over this area and during summer. This is also described by former studies. Lopez-Bustins and Lemus-Canovas (2020) found generally a dominant positive WeMO pattern during summer and a dominant negative WeMO pattern during winter, due to the decrease of the WeMO(−) influence during spring and summer, while the WeMO(+) influence only decreases during spring (Martinez-Artigas et al. 2021). Moreover, Merino et al. (2016) and Martinez-Artigas et al. (2021) reported a generally stronger influence of WeMO(+) conditions than WeMO(−) conditions over the northern IP, which additionally can be seen in figure 3.8a.

Over the central-southern zone of the IP (Fig. 3.14b), the mean area values reveal a clearer seasonal cycle than over the northern one, with a minimum in July and August. This can be explained by the weaker influence of the WeMO(−) during summer (Merino

et al. 2016; Martinez-Artigas et al. 2021; Lopez-Bustins et al. 2020; Lopez-Bustins and Lemus-Canovas 2020).

Annually, the area of EP occupied under WeMO(−) conditions is slightly greater than under a WeMO(+/0). However, the average monthly area during WeMOi(−) conditions exceeds those during WeMOi(+) conditions only in 6 months (September, November, January, March and April). In contrast to the northern zone, the differences between the mean areas under WeMOi(+) and WeMOi(−) conditions in the central-southern zone are generally greater in winter. It should be noted that in October and December, a higher mean area was found under a WeMOi(+), and not under a WeMOi(−) as expected. No literature was found to support this result. As already mentioned for the northern zone, these unexpected results may be caused by the calculation process and the fact that we used the monthly WeMOi for the daily EP.

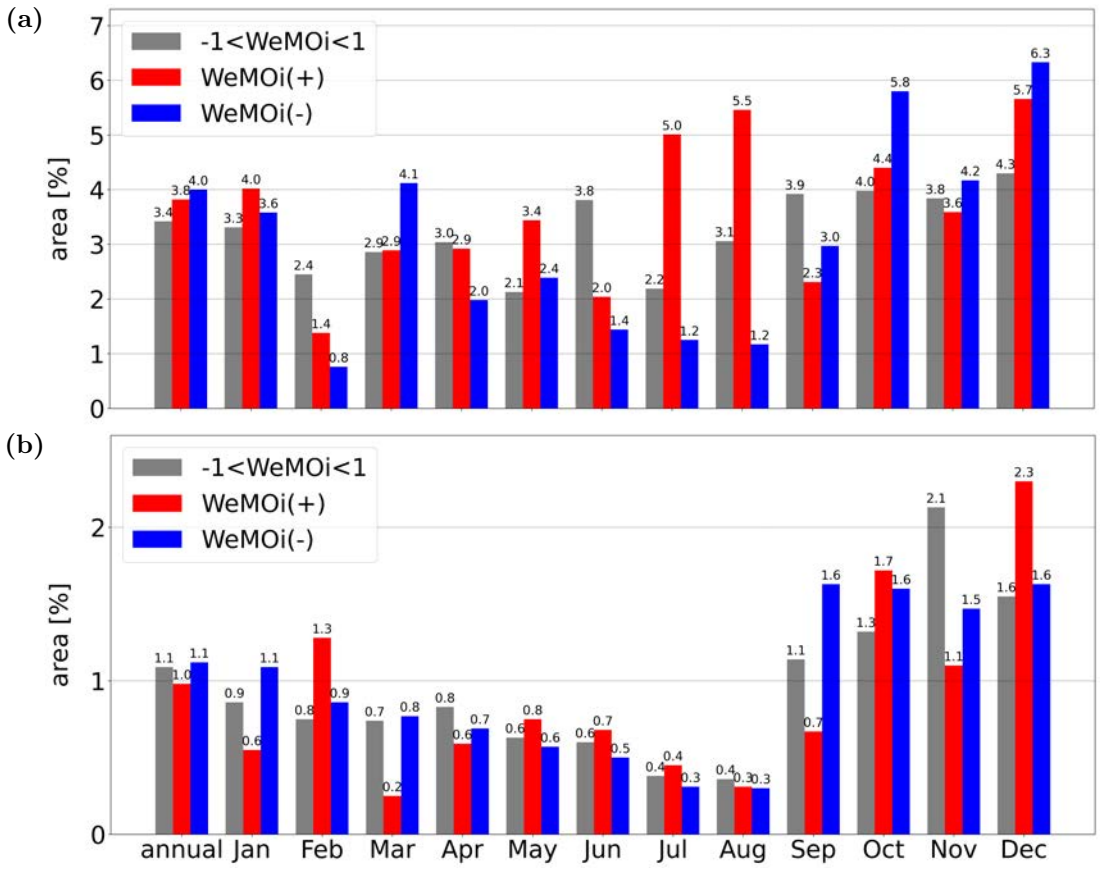

Figure 3.14: Mean area occupied by EP per month (in percentage) during the WeMOi(+/−/0) in the (a) northern zone and (b) central-southern zone. Period: 1980-2015. Note the different scales.

3.4.5 $|(E - P) < 0|$ for extreme precipitation and the WeMO

Furthermore, we computed the seasonal moisture contribution from each source for the areas occupied by EP events. The results, in figure 3.15, show the distribution of the moisture contribution to the extreme precipitation from each source over the northern and central-southern IP, concerning the total contribution (sum of the three sources), for the different seasons. In addition, changes in the moisture supply from these sources under WeMOi(+/−) conditions are displayed in figure 3.16.

As demonstrated in figure 3.9, once more, the NATL contributes the greater part of the moisture to the extreme precipitation over the northern and central-southern zones for all seasons ($\geq$ 73.0%), with its peak in the northern IP in summer (97.1%). Concerning the importance of moisture contribution to EP the NATL is followed by the MEDT and the IP for both zones and all seasons. This is supported by former studies. Vázquez et al. (2020) reported that throughout the year the NALT is the main source of EP over the IP, excluding the Mediterranean coast. Additionally, it was found that during peak precipitation months, the NATL plays the primary role of moisture source to precipitation over most of the IP. However, over the Mediterranean coast, the major source is the MEDT (Nieto et al. 2019; Vázquez et al. 2023). They also reported a switch of the MEDT and NATL sources concerning the role of the second most important source over most of the IP, except over the western IP, where it is the Gulf of Mexico and the Caribbean Sea (included in our NATL source). To confirm this, a spatial analysis is currently underway.

Furthermore, our analysis revealed that for the northern IP, the MEDT plays a more important role as a moisture source during winter and spring (approximately 25%) than during summer and autumn ($\leq$ 6.7%). Conversely, its importance for the central-southern IP is more balanced throughout the year (15.1-19.8%), except for spring. Later could be explained by the importance of the Mediterranean moisture source for EP in the eastern IP, which was reported in various articles (Nieto et al. 2019; Cloux et al. 2021; Insua-Costa et al. 2022; Vázquez et al. 2023). It appears that the importance of the MEDT is lower for all seasons over the central-southern zone than for winter and spring over the northern zone. Although, as mentioned in section 3.4.2, this is due to the relative analysis. However, in absolute values the highest $|(E - P) < 0|$ for EP from the MEDT is during JJA over the central-southern IP ($7.8e^{-3}$ mm day^{-1}), followed by MAM over the northern IP ($4.9e^{-3}$ mm day^{-1}) and by SON over the central-southern IP ($3.3e^{-3}$ mm day^{-1}).

Furthermore, the IP source itself plays a stronger role for the EP over the central-southern zone than over the northern one, with its highest importance during autumn for both zones (2.8% over the northern zone and 9.8% over the central-southern

zone). This was already observed in figure 3.9. However, in difference to the results from figure 3.9, in this analysis the IP contributes greater moisture to the EP also in absolute values during autumn concerning the other seasons ($0.4e^{-3}$ mm day^{-1} over the northern IP and $2.1e^{-3}$ mm day^{-1} over the central southern IP, Fig. S3.5)

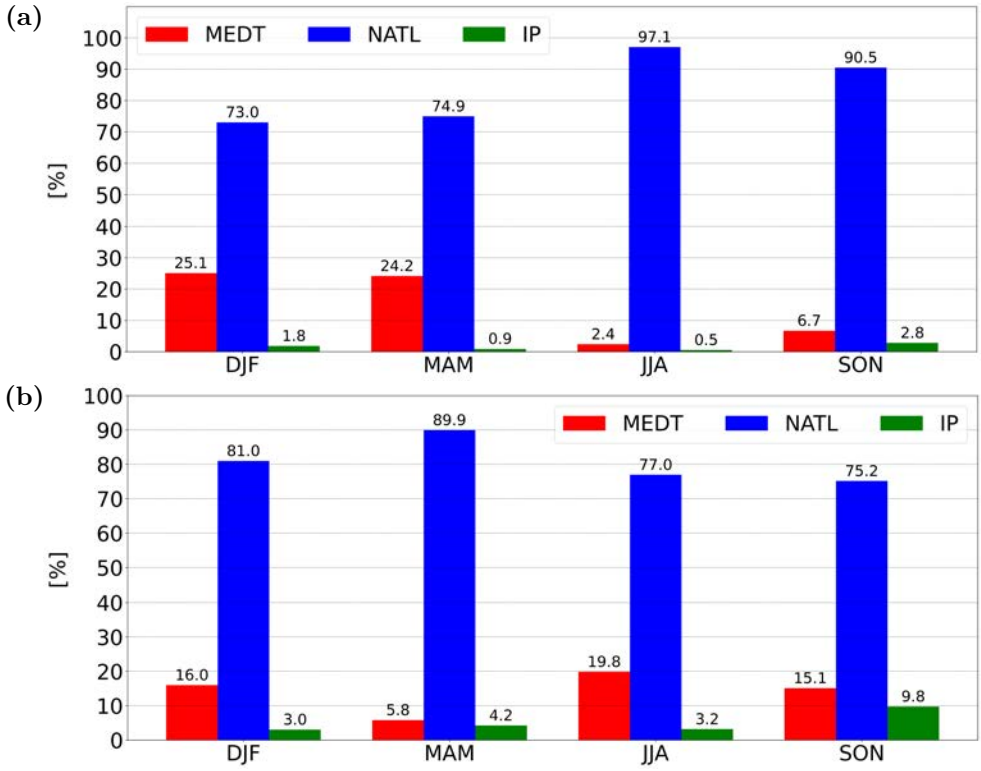

Figure 3.15: The mean moisture contributions to extreme precipitation (in percentage) from the MEDT (red), the NATL (blue) and the IP (green) to the IP. Period: 1980-2015. For winter (DJF), spring (MAM), summer (JJA) and autumn (SON), averaged over the (a) northern zone and (b) central-southern zone.

In terms of seasonal changes during the WeMO(+/−) phases (Fig. 3.16), during DJF in the northern and central-southern zone, the moisture contribution from the MEDT experienced a great reduction under the influence of the WeMO(+). At the same time, under a WeMOi(−), the MEDT increases its contribution drastically, principally in the central-southern zone. This is in agreement with the predominant moisture flux direction (Fig. 3.7a,b). In addition, the MEDT moisture source reveals great negative and drastic positive anomalies during positive and negative WeMO conditions in autumn over the northern zone, and in spring over the central-southern zone. Indeed, it has been demonstrated that WeMO(−) phases have a stronger influence on precipitation increase during winter over the central-southern zone, and during autumn over the northeastern IP (Martin-Vide and Lopez-Bustins 2006; Lopez-Bustins and Lemus-Canovas 2020; Lopez-Bustins et al. 2020; Martinez-Artigas et al. 2021). Consequently, when WeMO(−) phases get more frequent, the moisture transport from

the MEDT increases. Furthermore, $|(E - P) < 0|$ from the MEDT decreases during a WeMOi(+) for both zones and all seasons. For the central-southern zone, the values are fairly constant (-74.1 to -90.5%). Once more this can be explained by the WeMO(+) induced northwesterly atmospheric flow (Martin-Vide and Lopez-Bustins 2006; Lopez-Bustins et al. 2020; Martinez-Artigas et al. 2021), inhibiting the moisture flux from the MEDT.

The NATL moisture source for the IP changes less in percentage than the MEDT and IP during different WeMO phases. Thus, a weaker influence of the WeMO on the NATL moisture source for extreme precipitation could be assumed. However, a small increase in the contribution of the predominant source could play a more important role in the occurrence of EP than a large increase in the contribution of a source that climatologically contributes little moisture to the region. Positive changes in the NATL contribution can be observed over the northern IP under all WeMOi(+) and WeMOi($-$) conditions, except for SON under a WeMOi(+), and negative ones over the central-southern IP, except for JJA. Furthermore, during summer and autumn, it can be observed that $|(E - P) < 0|$ from the IP changes more with different WeMO conditions for both zones. However, no WeMO related pattern can be observed for the NATL and IP sources for extreme precipitation.

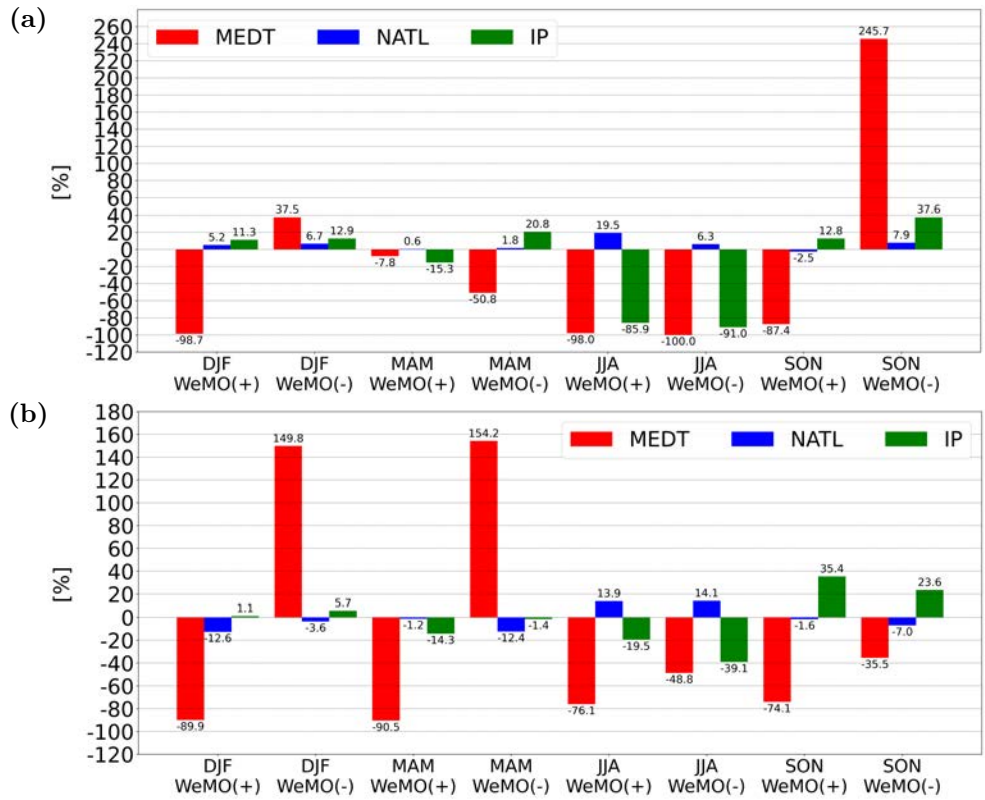

Figure 3.16: Changes in the mean moisture contributions to extreme precipitation (in percentage) from the MEDT (red), the NATL (blue) and the IP (green) to the IP. Period: 1980-2015. For winter (DJF), spring (MAM), summer (JJA) and autumn (SON), averaged over the (a) northern zone and (b) central-southern zone.

Chapter 4

Conclusions

In this study, we analysed, for the first time, the impact of the Western Mediterranean Oscillation (WeMO) on the moisture contributions from the North Atlantic Ocean (NATL) and the Mediterranean Sea (MEDT) to the precipitation patterns over Europe, for the period 1980-2018. Furthermore, it was studied in greater detail for the Iberian Peninsula (IP), including days with Extreme Precipitation (EP) and the contribution from the IP itself, as an additional moisture source, for 1980-2015. The Lagrangian FLEXible PARTicle dispersion model (FLEXPART) v9.0 was used to track the air masses forward in time from the source regions and to compute their contribution to the precipitation over the target regions, based on the negative values of integrated moisture loss in the budget of $|(E - P) < 0|$. In addition, various datasets were used to reach the aims of this study. After applying different mathematical and statistical analyses, various results were found, of which the most important are summarised and listed below:

- Precipitation over Europe is mostly positively correlated with the WeMOi, except for the central-southern IP, where an opposite linear relationship was found.

- The moisture contribution to precipitation from the MEDT is negatively (positively) correlated with the WeMOi over western (eastern) Europe. A similar correlation pattern as for the precipitation was obtained for the NATL moisture contribution, although it reveals less area with a negative relationship over the central-southern IP.

- The seasonal anomalies in the moisture contribution from the MEDT and NATL during positive WeMO phases generally lead to more precipitation over the areas from western-central to Eastern Europe, including the northern IP, parts of the Italian Peninsula and the Balkans.

- The seasonal anomalies in the moisture contribution from the MEDT and NATL during negative WeMO phases are related to more precipitation over the Western Mediterranean coast, including the Southern and Eastern IP.

- The WeMO has a stronger influence during autumn and winter, but the spatial configuration and sign of precipitation and $|(E - P) < 0|$ anomalies from the MEDT and NATL do not change significantly between different seasons.

- The response of precipitation over the IP to the influence of the WeMO(+/−) defines two zones with differentiated behaviour, the northern and the central-southern zone. A positive (negative) WeMO phase increases (decreases) the precipitation in the north (centre-south).

- For precipitation, as well as for the EP in both zones, NATL is the main source of moisture in all seasons, regardless of the WeMO phase.

- We found a statistically significant negative WeMO trend for the period 1980-2015. This is accompanied by a negative precipitation trend, a negative $|(E - P) < 0|$ from the MEDT trend and a statistically significant positive $|(E-P) < 0|$ from the NATL trend over the northern zone of the IP. In addition, the analysis, over the central-southern zone of the IP, resulted in positive trends for all three variables.

- The WeMO explains the frequency of occurrence of EP days better than the area they occupy. In the northern IP, more days with extreme precipitation take place during WeMO(+), while in the central-southern IP, it occurs during WeMO(−), particularly in winter.

- The moisture contribution to extreme precipitation from the MEDT changes more than from the NATL or the IP, regarding the different WeMO phases .

The above listed results reveal and confirm that the WeMO plays a relevant impact on moisture transport from the MEDT and NATL, and consequently to the precipitation over Europe, particularly the IP. The analysis carried out over more than 30 years ensures reliable results, and contributes to the understanding of the ocean-atmosphere-land interaction, and thus of the hydrological cycle on our planet. It also provides important information for weather and climate prediction, supporting environmental and socio-economic activities. To continue and deepen this work, we plan to investigate the behaviour of WeMO in future scenarios under climate change conditions. This will allow us to determine its role in possible changes in moisture transport from the sources compared to the historical period and the impact on the precipitation over Europe. In addition, we also plan to consider other modes of climate variability. Future studies of the WeMO and extreme precipitation events should consider the daily WeMOi.

Acknowledgements

I would like to extend my sincere gratitude to the EPhysLab and my two advisors, Dr. Rogert Sorí Gómez and Dr. Milica Stojanovic, for their invaluable help, support, and guidance throughout this research project. Their expertise and encouragement have significantly enhanced my understanding of science and meteorology. In addition, I want to thank María, Elisa and Rocío, who spent their free time giving me advice, and María for correcting my English spelling in the last hours. I would also like to express my heartfelt thanks to my friends in Vigo, who warmly welcomed me and integrated me into the Spanish lifestyle, fostering a strong and profound friendship. My deepest appreciation goes to my family for their unwavering support, even when my studies took me far from home to Spain. I also acknowledge the support of this Master's Thesis with a PDI contract in the University of Vigo, financed by the project RYC2021-034044-I which was financed by MICIU/AEI/10.13039/501100011033 and the European Union "NextGenerationEU"/PRTR. This work was possible because of the computing resources and technical support provided by the Centro de Supercomputación de Galicia (CESGA).

Bibliography

Batibeniz, F., M. Ashfaq, B. Önol, U. Turuncoglu, S. Mehmood, and K. Evans, 2020: Identification of major moisture sources across the Mediterranean Basin. *Climate Dynamics*, **54**, 1–19, doi:10.1007/s00382-020-05224-3.

Benetó, P. and S. Khodayar, 2023: On the need for improved knowledge on the regional-to-local precipitation variability in eastern Spain under climate change. *Atmospheric Research*, **290**, 106 795, doi:10.1016/j.atmosres.2023.106795.

Cardoso Pereira, S., M. Marta-Almeida, A. C. Carvalho, and A. Rocha, 2020: Extreme precipitation events under climate change in the Iberian Peninsula. *International Journal of Climatology*, **40 (2)**, 1255–1278, doi:10.1002/joc.6269.

Casanueva, A., C. Rodríguez-Puebla, M. D. Frías, and N. González-Reviriego, 2014: Variability of extreme precipitation over Europe and its relationships with teleconnection patterns. *Hydrology and Earth System Sciences*, **18 (2)**, 709–725, doi:10.5194/hess-18-709-2014.

Castillo, R., R. Nieto, A. Drumond, and L. Gimeno, 2014: The role of the ENSO cycle in the modulation of moisture transport from major oceanic moisture sources. *Water Resources Research*, **50 (2)**, 1046–1058, doi:10.1002/2013WR013900.

Cloux, S., D. Garaboa-Paz, D. Insua-Costa, G. Miguez-Macho, and V. Pérez-Muñuzuri, 2021: Extreme precipitation events in the Mediterranean area: contrasting two different models for moisture source identification. *Hydrology and Earth System Sciences*, **25 (12)**, 6465–6477, doi:10.5194/hess-25-6465-2021.

Cornes, R. C., G. van der Schrier, E. J. M. van den Besselaar, and P. D. Jones, 2018: An Ensemble Version of the E-OBS Temperature and Precipitation Data Sets. *Journal of Geophysical Research: Atmospheres*, **123 (17)**, 9391–9409, doi:10.1029/2017JD028200.

Cos, J., F. Doblas-Reyes, M. Jury, R. Marcos, P.-A. Bretonnière, and M. Samsó, 2022: The Mediterranean climate change hotspot in the CMIP5 and CMIP6 projections. *Earth System Dynamics*, **13 (1)**, 321–340, doi:10.5194/esd-13-321-2022.

Dee, D. P., et al., 2011: The ERA-Interim reanalysis: configuration and performance of the data assimilation system. *Quarterly Journal of the Royal Meteorological Society*, **137 (656)**, 553–597, doi:10.1002/qj.828.

Devanand, A., et al., 2024: Australia's Tinderbox Drought: An extreme natural event likely worsened by human-caused climate change. *Science Advances*, **10 (10)**, eadj3460, doi:10.1126/sciadv.adj3460.

Dirmeyer, P. A. and K. L. Brubaker, 1999: Contrasting evaporative moisture sources during the drought of 1988 and the flood of 1993. *Journal of Geophysical Research: Atmospheres*, **104 (D16)**, 19 383–19 397, doi:10.1029/1999JD900222.

Dirmeyer, P. A. and K. L. Brubaker, 2006: Evidence for trends in the Northern Hemisphere water cycle. *Geophysical Research Letters*, **33 (14)**, doi:10.1029/2006GL026359.

Dong, B., R. T. Sutton, T. Woollings, and K. Hodges, 2013: Variability of the North Atlantic summer storm track: mechanisms and impacts on European climate. *Environmental Research Letters*, **8 (3)**, 034 037, doi:10.1088/1748-9326/8/3/034037.

Egger, A. E., 2003: The Hydrologic Cycle: Reservoirs and fluxes of water on Earth. Visionlearning Vol. EAS-2 (2), Accessed online at: www.visionlearning.com/en/library/Earth-Science/6/The-Hydrologic-Cycle/99/reading on June 13, 2024.

European Environment Agency, 2021: *Water resources across Europe – Confronting water stress: an updated assessment*. Publications Office of the European Union, doi:doi/10.2800/320975.

Fernández-Alvarez, J. C., A. Pérez-Alarcón, J. Eiras-Barca, S. Rahimi, R. Nieto, and L. Gimeno, 2023: Projected changes in atmospheric moisture transport contributions associated with climate warming in the North Atlantic. *Nature Communications*, **14**, doi:10.1038/s41467-023-41915-1.

Gimeno, L., 2013: Grand challenges in atmospheric science. *Frontiers in Earth Science*, **1**, doi:10.3389/feart.2013.00001.

Gimeno, L., A. Drumond, R. Nieto, R. M. Trigo, and A. Stohl, 2010a: On the origin of continental precipitation. *Geophysical Research Letters*, **37 (13)**, doi:10.1029/2010GL043712.

Gimeno, L., R. Nieto, A. Drumond, A. M. Durán-Quesada, A. Stohl, H. Sodemann, and R. M. Trigo, 2011: A close look at oceanic sources of continental precipitation. *Eos, Transactions American Geophysical Union*, **92 (23)**, 193–194, doi:10.1029/2011EO230001.

Gimeno, L., R. Nieto, R. M. Trigo, S. M. Vicente-Serrano, and J. I. López-Moreno, 2010b: Where Does the Iberian Peninsula Moisture Come From? An Answer Based

on a Lagrangian Approach. *Journal of Hydrometeorology*, **11 (2)**, 421 – 436, doi: 10.1175/2009JHM1182.1.

Gimeno, L., R. Sorí, M. Vázquez, M. Stojanovic, I. Algarra, J. Eiras-Barca, L. Gimeno-Sotelo, and R. Nieto, 2022: Extreme precipitation events. *WIREs Water*, **9 (6)**, e1611, doi:10.1002/wat2.1611.

Gimeno, L., et al., 2012: Oceanic and terrestrial sources of continental precipitation. *Reviews of Geophysics*, **50 (4)**, doi:10.1029/2012RG000389.

Gimeno, L., et al., 2021: The residence time of water vapour in the atmosphere. *Nature Reviews Earth & Environment*, **2**, doi:10.1038/s43017-021-00181-9.

Gimeno-Sotelo, L., R. Sorí, R. Nieto, S. Vicente-Serrano, and L. Gimeno, 2024a: Unravelling the origin of the atmospheric moisture deficit that leads to droughts. *Nature Water*, **2**, 242–253, doi:10.1038/s44221-023-00192-4.

Gimeno-Sotelo, L., M. Stojanovic, R. Sori, R. Nieto, S. M. Vicente-Serrano, and L. Gimeno, 2024b: Nexus between the deficit in moisture transport and drought occurrence in regions with projected drought trends. *Environmental Research Letters*, 074035, doi:10.1088/1748-9326/ad560b.

Gómez-Hernández, M., A. Drumond, L. Gimeno, and R. Garcia-Herrera, 2013: Variability of moisture sources in the Mediterranean region during the period 1980–2000. *Water Resources Research*, **49 (10)**, 6781–6794, doi:10.1002/wrcr.20538.

Herrera, S., R. M. Cardoso, P. M. Soares, F. Espírito-Santo, P. Viterbo, and J. M. Gutiérrez, 2019: Iberia01: a new gridded dataset of daily precipitation and temperatures over Iberia. *Earth System Science Data*, **11 (4)**, 1947–1956, doi: 10.5194/essd-11-1947-2019.

Herrera-Estrada, J. E. and N. S. Diffenbaugh, 2020: Landfalling Droughts: Global Tracking of Moisture Deficits From the Oceans Onto Land. *Water Resources Research*, **56 (9)**, doi:10.1029/2019WR026877.

Hersbach, H., et al., 2023: ERA5 monthly averaged data on single levels from 1940 to present. *Copernicus Climate Change Service (C3S) Climate Data Store (CDS)*, doi:10.24381/cds.f17050d7.

Horan, M., F. Batibeniz, F. Kucharski, M. Almazroui, M. A. Abid, J. Fu, and M. Ashfaq, 2023: Moisture sources for precipitation variability over the Arabian Peninsula. *Climate Dynamics*, **61**, 1–15, doi:10.1007/s00382-023-06762-2.

Insua-Costa, D., M. Senande-Rivera, M. Llasat, and G. Miguez-Macho, 2022: A global perspective on western Mediterranean precipitation extremes. *npj Climate and Atmospheric Science*, **5**, doi:10.1038/s41612-022-00234-w.

Kozachek, A., et al., 2017: Large-scale drivers of Caucasus climate variability in meteorological records and Mt El'brus ice cores. *Climate of the Past*, **13**, 473–489, doi:10.5194/cp-13-473-2017.

Liu, B., X. Tan, T. Y. Gan, X. Chen, K. Lin, M. Lu, and Z. Liu, 2020: Global atmospheric moisture transport associated with precipitation extremes: Mechanisms and climate change impacts. *WIREs Water*, **7 (2)**, e1412, doi:10.1002/wat2.1412.

Lopez-Bustins, J. A., L. Arbiol-Roca, J. Martin-Vide, A. Barrera-Escoda, and M. Prohom, 2020: Intra-annual variability of the Western Mediterranean Oscillation (WeMO) and occurrence of extreme torrential precipitation in Catalonia (NE Iberia). *Natural Hazards and Earth System Sciences*, **20 (9)**, 2483–2501, doi:10.5194/nhess-20-2483-2020.

Lopez-Bustins, J. A. and M. Lemus-Canovas, 2020: The influence of the Western Mediterranean Oscillation upon the spatio-temporal variability of precipitation over Catalonia (northeastern of the Iberian Peninsula). *Atmospheric Research*, **236**, 104 819, doi:10.1016/j.atmosres.2019.104819.

Lopez-Bustins, J.-A., J. Martin-Vide, and A. Sanchez-Lorenzo, 2008: Iberia winter rainfall trends based upon changes in teleconnection and circulation patterns. *Global and Planetary Change*, **63 (2)**, 171–176, doi:10.1016/j.gloplacha.2007.09.002.

Luo, D., Z. Hu, L. Dai, G. Hou, K. Di, M. Liang, R. Cao, and X. Zeng, 2023: An overall consistent increase of global aridity in 1970–2018. *Journal of Geographical Sciences*, **33**, 449–463, doi:10.1007/s11442-023-2091-0.

Ma, J., et al., 2020: Hydrological cycle changes under global warming and their effects on multiscale climate variability. *Annals of the New York Academy of Sciences*, **1472 (1)**, 21–48, doi:10.1111/nyas.14335.

Mariotti, A., M. V. Struglia, N. Zeng, and K.-M. Lau, 2002: The Hydrological Cycle in the Mediterranean Region and Implications for the Water Budget of the Mediterranean Sea. *Journal of Climate*, **15 (13)**, 1674 – 1690, doi:10.1175/1520-0442(2002)015⟨1674:THCITM⟩2.0.CO;2.

Martin-Vide, J. and J.-A. Lopez-Bustins, 2006: The Western Mediterranean Oscillation and rainfall in the Iberian Peninsula. *International Journal of Climatology*, **26 (11)**, 1455–1475, doi:10.1002/joc.1388.

Martinez-Artigas, J., M. Lemus-Canovas, and J. A. Lopez-Bustins, 2021: Precipitation in peninsular Spain: Influence of teleconnection indices and spatial regionalisation. *International Journal of Climatology*, **41 (S1)**, E1320–E1335, doi:10.1002/joc.6770.

Merino, A., M. Fernández-Vaquero, L. López, S. Fernández-González, L. Hermida, J. L. Sánchez, E. García-Ortega, and E. Gascón, 2016: Large-scale patterns of daily precipitation extremes on the Iberian Peninsula. *International Journal of Climatology*, **36 (11)**, 3873–3891, doi:10.1002/joc.4601.

Nieto, R., R. Castillo, A. Drumond, and L. Gimeno, 2014: A catalog of moisture sources for continental climatic regions. *Water Resources Research*, **50 (6)**, 5322–5328, doi:10.1002/2013WR013901.

Nieto, R., D. Ciric, M. Vázquez, M. L. Liberato, and L. Gimeno, 2019: Contribution of the main moisture sources to precipitation during extreme peak precipitation months. *Advances in Water Resources*, **131**, 103 385, doi:10.1016/j.advwatres.2019.103385.

Nieto, R., L. Gimeno, A. Drumond, and E. Hernández, 2010: A Lagrangian identification of the main moisture sources and sinks affecting the Mediterranean area. *WSEAS Transactions on Environment and Development*, **6 (5)**, 365–374, ISSN:1790-5079.

Numaguti, A., 1999: Origin and recycling processes of precipitating water over the eurasian continent: Experiments using an atmospheric general circulation model. *Journal of Geophysical Research: Atmospheres*, **104 (D2)**, 1957–1972, doi:10.1029/1998JD200026.

Oki, T. and S. Kanae, 2006: Global hydrological cycles and world water resources. *Science (New York, N.Y.)*, **313**, 1068–72, doi:10.1126/science.1128845.

Ordóñez, P., M. L. R. Liberato, C. Gouveia, and R. M. Trigo, 2013: North Atlantic Oscillation and moisture transport towards the Iberian Peninsula during winter. *EGU General Assembly Conference Abstracts*, EGU2013–12 058, EGU General Assembly Conference Abstracts, Accessed online at:https://ui.adsabs.harvard.edu/abs/2013EGUGA..1512058O on July 14, 2024.

Pereira, S. C., D. Carvalho, and A. Rocha, 2021: Temperature and Precipitation Extremes over the Iberian Peninsula under Climate Change Scenarios: A Review. *Climate*, **9 (9)**, doi:10.3390/cli9090139.

Pérez-Alarcón, A., R. Sorí, J. C. Fernández-Alvarez, R. Nieto, and L. Gimeno, 2022: Where Does the Moisture for North Atlantic Tropical Cyclones Come From? *Journal of Hydrometeorology*, **23 (3)**, 457 – 472, doi:10.1175/JHM-D-21-0117.1.

Quante, M. and V. Matthias, 2006: Water in the Earth's atmosphere. *J. Phys. IV France*, **139**, 37–61, doi:10.1051/jp4:2006139005.

Rios-Entenza, A., P. M. M. Soares, R. M. Trigo, R. M. Cardoso, and G. Miguez-Macho, 2014: Moisture recycling in the Iberian Peninsula from a regional climate simulation: Spatiotemporal analysis and impact on the precipitation regime. *Journal of Geophysical Research: Atmospheres*, **119 (10)**, 5895–5912, doi:10.1002/2013JD021274.

Schulzweida, U., 2023: CDO User Guide. Zenodo, doi:10.5281/zenodo.10020800.

Seager, R., H. Liu, Y. Kushnir, T. J. Osborn, I. R. Simpson, C. R. Kelley, and J. Nakamura, 2020: "mechanisms of winter precipitation variability in the european–mediterranean region associated with the north atlantic oscillation". *Journal of Climate*, **33 (16)**, 7179 – 7196, doi:10.1175/JCLI-D-20-0011.1.

Senent-Aparicio, J., A. López-Ballesteros, P. Jimeno-Sáez, and J. Pérez-Sánchez, 2023: Recent precipitation trends in Peninsular Spain and implications for water infrastructure design. *Journal of Hydrology: Regional Studies*, **45**, 101 308, doi:10.1016/j.ejrh.2022.101308.

Seneviratne, S., et al., 2021: Weather and Climate Extreme Events in a Changing Climate. *Climate Change 2021: The Physical Science Basis. Contribution of Working Group I to the Sixth Assessment Report of the Intergovernmental Panel on Climate Change*, V. Masson-Delmotte, P. Zhai, A. Pirani, S. Connors, C. Péan, S. Berger, N. Caud, Y. Chen, L. Goldfarb, M. Gomis, M. Huang, K. Leitzell, E. Lonnoy, J. Matthews, T. Maycock, T. Waterfield, O. Yelekçi, R. Yu, and B. Zhou, Eds., Cambridge University Press, Cambridge, United Kingdom and New York, NY, USA, 1513–1766, doi:10.1017/9781009157896.013.

Shahi, N., J. Polcher, S. Bastin, R. Pennel, and L. Fita, 2022: Assessment of the spatio-temporal variability of the added value on precipitation of convection-permitting simulation over the Iberian Peninsula using the RegIPSL regional earth system model. *Climate Dynamics*, 471–498, doi:10.1007/s00382-022-06138-y.

Shaman, J., 2014: The Seasonal Effects of ENSO on European Precipitation: Observational Analysis. *Journal of Climate*, **27 (17)**, 6423 – 6438, doi:10.1175/JCLI-D-14-00008.1.

Smith, A., P. Wynn, P. Barker, M. Leng, S. Noble, and W. Tych, 2016: North Atlantic forcing of moisture delivery to Europe throughout the Holocene. *Scientific Reports*, **6**, doi:10.1038/srep24745.

Soden, B., 2019: Progress and Challenges in Understanding the Atmospheric Hydrological Cycle. *AGU Fall Meeting Abstracts*, Vol. 2019, A11C–02, Accessed online at: https://ui.adsabs.harvard.edu/abs/2019AGUFM.A11C..02S/abstract on July 14, 2024.

Sorí, R., L. Gimeno-Sotelo, R. Nieto, M. L. Liberato, M. Stojanovic, A. Pérez-Alarcón, J. C. Fernández-Alvarez, and L. Gimeno, 2023: Oceanic and terrestrial origin of precipitation over 50 major world river basins: Implications for the occurrence of drought. *Science of The Total Environment*, **859**, 160 288, doi:10.1016/j.scitotenv.2022.160288.

Stohl, A. and P. James, 2004: A Lagrangian Analysis of the Atmospheric Branch of the Global Water Cycle. Part I: Method Description, Validation, and Demonstration for the August 2002 Flooding in Central Europe. *Journal of Hydrometeorology*, **5 (4)**, 656 – 678, doi:10.1175/1525-7541(2004)005⟨0656:ALAOTA⟩2.0.CO;2.

Stohl, A. and P. James, 2005: A Lagrangian Analysis of the Atmospheric Branch of the Global Water Cycle. Part II: Moisture Transports between Earth's Ocean Basins and River Catchments. *Journal of Hydrometeorology*, **6 (6)**, 961 – 984, doi:10.1175/JHM470.1.

Sánchez Gómez, E., S. Somot, S. Josey, C. Dubois, N. Elguindi, and M. Déqué, 2009: Evaluation of Mediterranean Sea water and heat budgets simulated by an ensemble of high resolution regional climate models. *Climate Dynamics*, **37**, 2067–2086, doi:10.1007/s00382-011-1012-6.

Tabari, H. and P. Willems, 2018: Lagged influence of Atlantic and Pacific climate patterns on European extreme precipitation. *Scientific Reports*, **8**, doi:10.1038/s41598-018-24069-9.

Ullah, S., Q. You, D. Sachindra, M. Nowosad, W. Ullah, A. S. Bhatti, Z. Jin, and A. Ali, 2022: Spatiotemporal changes in global aridity in terms of multiple aridity indices: An assessment based on the CRU data. *Atmospheric Research*, **268**, 105 998, doi:10.1016/j.atmosres.2021.105998.

Van Rossum, G. and F. L. Drake, 2009: *Python 3 Reference Manual*. CreateSpace, Scotts Valley, CA, ISBN:1441412697.

Virtanen, P., et al., 2020: SciPy 1.0: Fundamental Algorithms for Scientific Computing in Python. *Nature Methods*, **17**, 261–272, doi:10.1038/s41592-019-0686-2.

Vázquez, M., F. Ferreira, R. Nieto, M. Liberato, and L. Gimeno, 2020: Moisture Transport toward Europe and Extreme Precipitation Events. *in Proceedings of the 3rd In-*

ternational Electronic Conference on Atmospheric Sciences, MDPI: Basel, Switzerland, doi:10.3390/ecas2020-08137.

Vázquez, M., R. Nieto, M. L. R. Liberato, and L. Gimeno, 2023: Influence of teleconnection patterns on global moisture transport during peak precipitation month. *International Journal of Climatology*, **43 (2)**, 932–949, doi:10.1002/joc.7843.

Walsh, J. E. and D. H. Portis, 1999: Variations of precipitation and evaporation over the North Atlantic Ocean, 1958–1997. *Journal of Geophysical Research: Atmospheres*, **104 (D14)**, 16 613–16 631, doi:10.1029/1999JD900189.

Watterson, I. G., 2023: Atmospheric Moisture Transport Associated with Precipitation in Present and Simulated Future Climates. *Journal of Climate*, **36 (18)**, 6409 – 6425, doi:10.1175/JCLI-D-22-0588.1.

Wypych, A., B. Bochenek, and M. Różycki, 2018: Atmospheric Moisture Content over Europe and the Northern Atlantic. *Atmosphere*, **9 (1)**, doi:10.3390/atmos9010018.

Yang, Y., et al., 2022: Moisture Transport and Contribution to the Continental Precipitation. *Atmosphere*, **13 (10)**, doi:10.3390/atmos13101694.

Zveryaev, I. and A. Hannachi, 2022: Inter-Annual Variability of Mediterranean Evaporation and Its Drivers During Summer. *New Prospects in Environmental Geosciences and Hydrogeosciences*, H. Chenchouni, H. I. Chaminé, M. F. Khan, B. J. Merkel, Z. Zhang, P. Li, A. Kallel, and N. Khélifi, Eds., Springer International Publishing, Cham, 25–28, doi:10.1007/978-3-030-72543-3_6.

Önol, B., D. Bozkurt, O. Sen, and N. Dalfes, 2014: Evaluation of the twenty-first century RCM simulations driven by multiple GCMs over the Eastern Mediterranean-Black Sea region. *Climate Dynamics*, **42**, 1949–1965, doi:10.1007/s00382-013-1966-7.

Supplementary Material

Figures

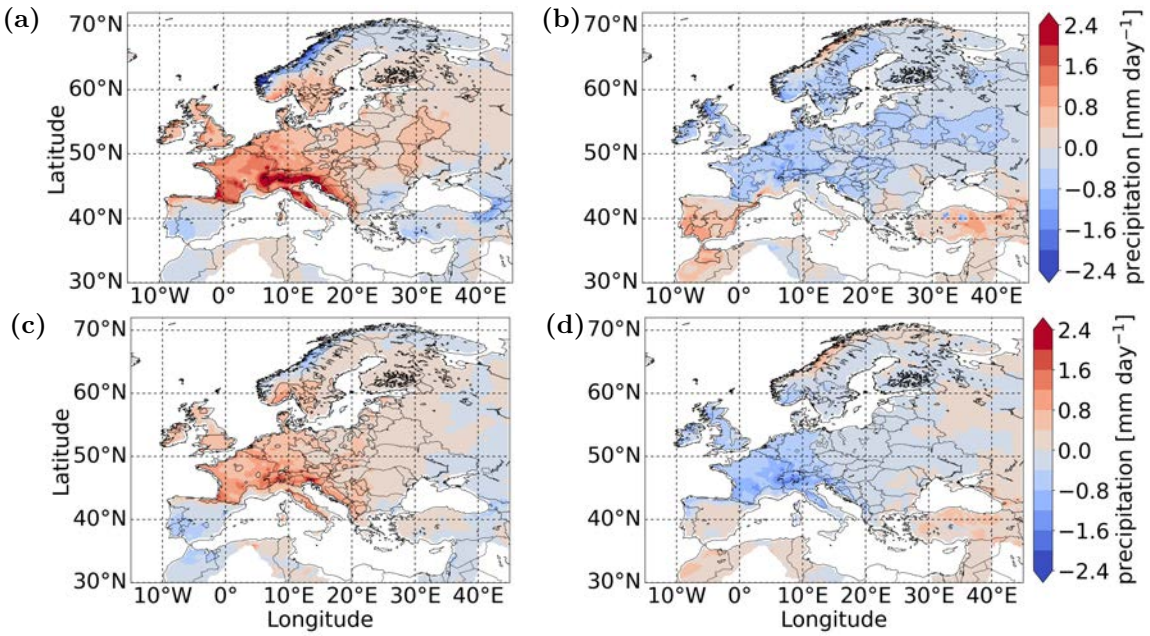

Figure S3.1: Anomalies of precipitation during SON (top) and MAM (bottom) under the influence of positive (left column) and negative (right column) of WeMOi phases, 1980-2018. Dashed/solid black lines delimit areas with statistically significant ($p < 0.05$) values.

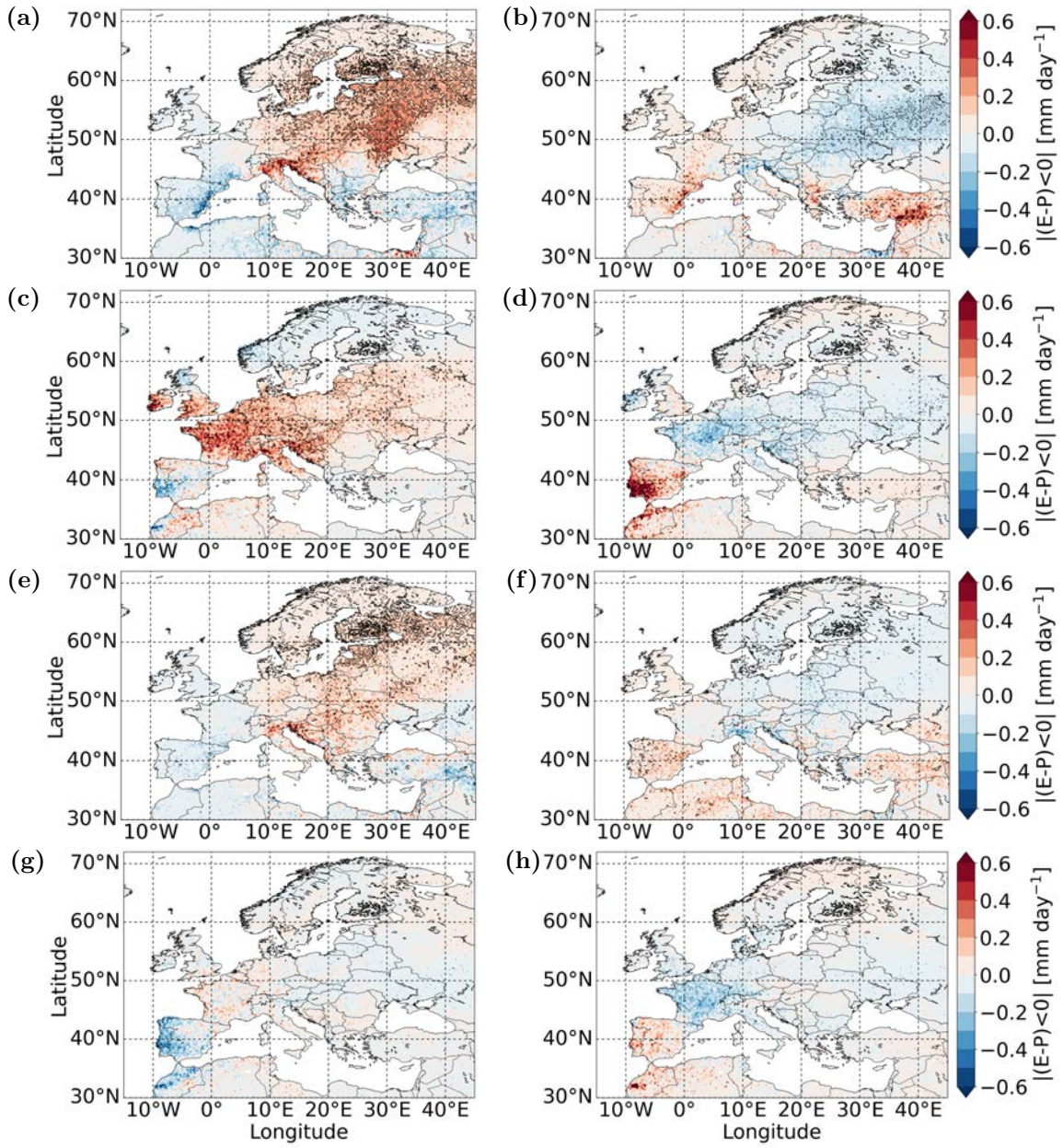

Figure S3.2: Anomalies of the moisture contribution to precipitation from the MEDT and NATL during WeMOi(+/−). Period: 1980-2018. The left column represents anomalies during WeMOi(+) and the right column represents anomalies during WeMOi(−). (a,b) represent the DJF anomalies on the contribution from the MEDT and (c,d) from the NATL. (e,f) represent the JJA anomalies on the contribution from the MEDT and (g,h) from the NATL. Dashed/solid black lines indicate statistically significant ($p < 0.05$) values.

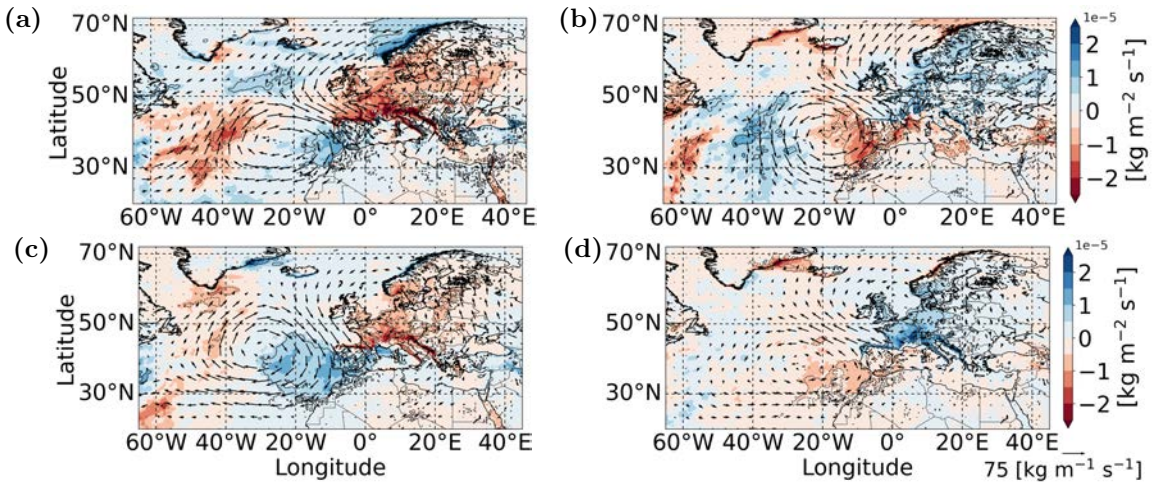

Figure S3.3: Anomalies of the VIMF during DJF (top) and JJA (bottom) under the influence of positive (left column) and negative (right column) of WeMOi phases, 1980-2018. Dashed/solid black lines delimit VIMF divergence areas with statistically significant ($p < 0.05$) values, arrows indicate VIMF anomalies.

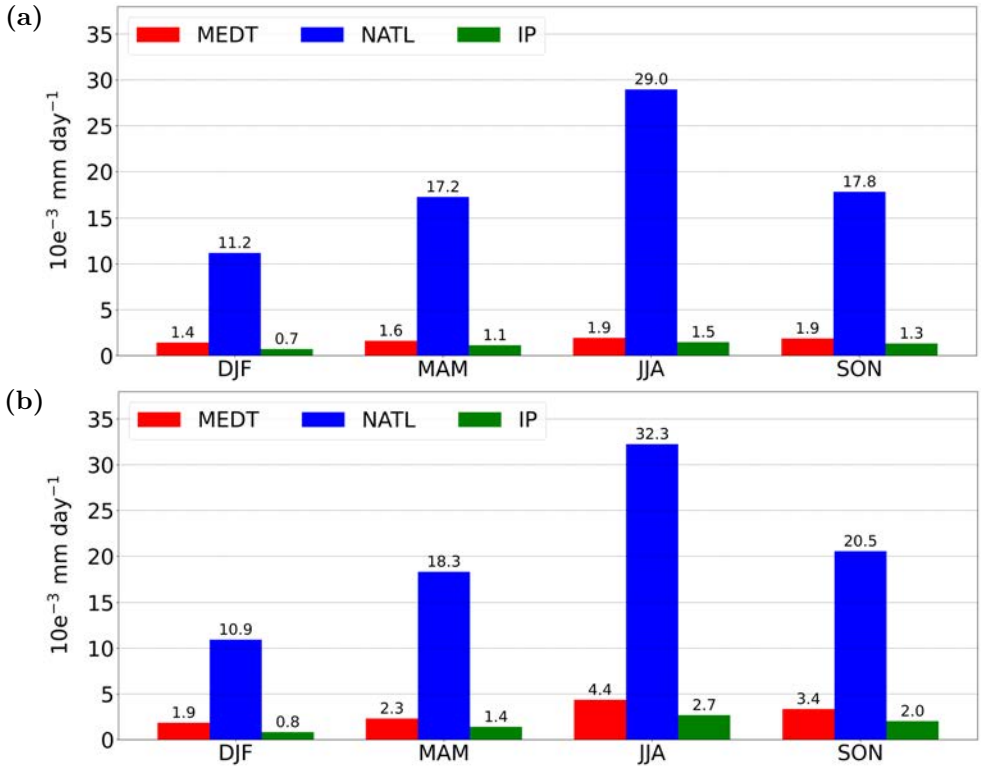

Figure S3.4: The mean moisture contributions to precipitation (in percentage) from the MEDT (red), the NATL (blue) and the IP (green) to the IP. Period: 1980-2015. For winter (DJF), spring (MAM), summer (JJA) and autumn (SON), averaged over the (a) northern zone and (b) central-southern zone.

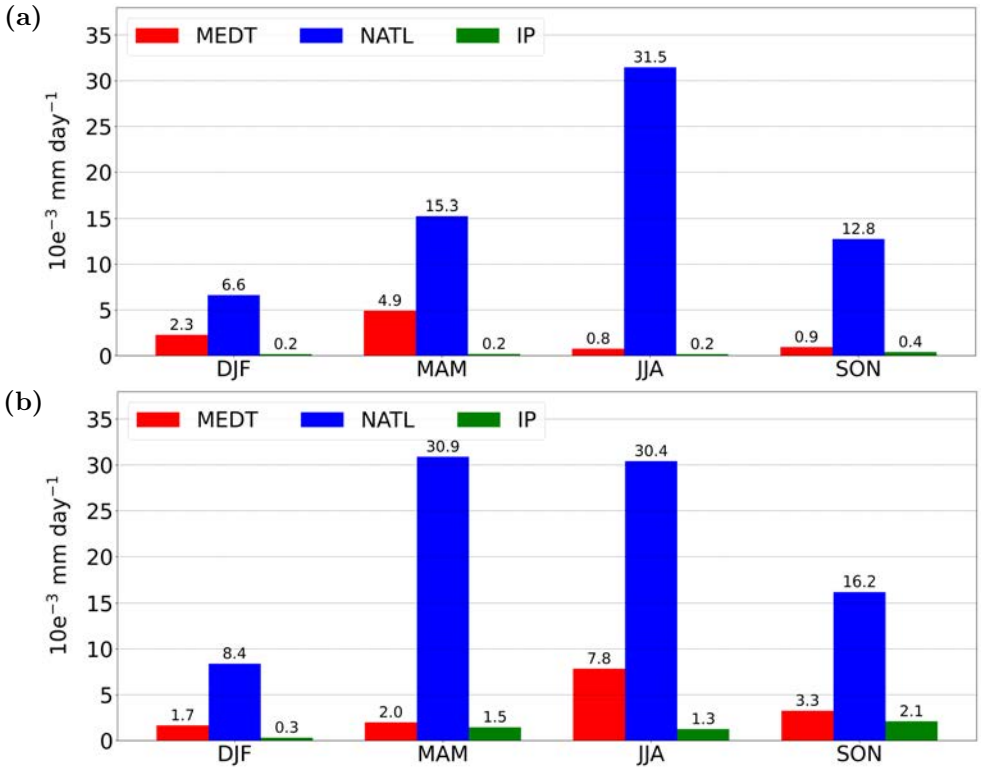

Figure S3.5: The mean moisture contributions to extreme precipitation (in percentage) from the MEDT (red), the NATL (blue) and the IP (green) to the IP. Period: 1980-2015. For winter (DJF), spring (MAM), summer (JJA) and autumn (SON), averaged over the (a) northern zone and (b) central-southern zone.